ARTHUR D. LITTLE, INC.
15 Acorn Park
Cambridge, Massachusetts 02140

THERMODYNAMICS OF CONDENSED AND VAPOR PHASES IN THE BINARY AND TERNARY SYSTEMS OF Be-B-O, Al-B-O, Si-O, Al-Be-O AND Al-B-F

By

Paul E. Blackburn

For

Office of Aerospace Research

FINAL REPORT

May 31, 1965

ARPA Project Code No. 9100
ARPA Order No. 315-62

TABLE OF CONTENTS

LIST OF FIGURES

LIST OF TABLES

THERMODYNAMICS OF CONDENSED AND VAPOR PHASES IN THE BINARY AND TERNARY SYSTEMS OF Be-B-O, Al-B-O, Si-O, Al-Be-O and Al-B-F

ABSTRACT

Thermodynamic properties of binary and ternary vapor and condensed systems were obtained by measuring pressures by the Knudsen and Langmuir methods. Vacuum balances and a mass spectrometer were used in these studies.

An evaporation coefficient $\alpha_e = 3 \times 10^{-2}$ was found for $B_2O_3(\ell)$. A third-law heat of vaporization $\Delta H_{298} = 99.2 \pm 0.4$ kcal/mole and second-law heat $\Delta H_{298} = 99.6 \pm 1.6$ kcal/mole of $B_2O_3(g)$ were measured. Experiments on $SiO_2(\ell)$ gave $\alpha_e = 5 \times 10^{-3}$ and $\Delta H_f^\circ 298 = -22.6 \pm 1.0$ kcal/mole SiO(g).

In the Be-B-O system only one condensed mixed phase exists, $Be_3B_2O_6(c)$ with a melting point of 1495 ± 5°C. $Be(BO_2)_2(g)$ has an entropy at 1500°K $S_{1500} = 127$ eu and heat of formation $\Delta H_f^\circ 1500 = -324$ kcal/mole. The same properties for $Be_3B_2O_6$ are $S_{1500} = 108$ eu and $\Delta H_f^\circ 1500 = -745$ kcal/mole.

In the Al-B-O system, $Al_4B_2O_9(c)$ has $\Delta H_f^\circ(1200) = -1114$ kcal/mole, and $S_{1200} = 154$ eu/mole. In $Al_{18}B_4O_{33}(c)$, $\Delta H_f 1500 = -4251$ kcal/mole and $S_{1500} = 607$ eu/mole. Only B_2O_3 vapor was found over the four pseudo-binary systems: $B_2O_3(\ell)$-$Al_4B_2O_9(c)$, $Al_4B_2O_9$-$Al_{18}B_4O_{33}$, $B_2O_3(\ell)$-$Al_{18}B_4O_{33}$ and $Al_{18}B_4O_{33}$-Al_2O_3. A mixture of $B_2O_3 + Al_2O_3 + Al$ produced the previously known species: Al(g), BO, B_2O_2, Al_2O and B_2O_3. One metaborate, $AlBO_2(g)$ was found with $\Delta H_f^\circ 1500 = -140 \pm 4$ kcal/mole.

Vapor pressures of rhenium gave a heat of vaporization ΔH°_{298} = 184.5 + 1.5 kcal/g-atom.

Effusion measurements on $Al_2O_3(\ell)$ were in excellent agreement with data calculated from Drowart et al.[32] Langmuir measurements above and below the melting point of Al_2O_3 failed to produce the discontinuity in evaporation rates claimed by Burns et al.[33] The evaporation coefficient of both liquid and crystalline alumina is found to be in excess of 0.5.

Effusion measurements on BeO are in excellent agreement with Chupka et al.[31] confirming their calculation of the ratios of $(BeO)_n$ molecules to Be and O atoms.

$BeO.3Al_2O_3(\ell)$ was found to vaporize congruently at 2415°K. A heat of formation of this compound ΔH_{298} = -54 ± 15 kcal/mole from the oxides was found. Using Efimenko's[39] mass spectrometric data and this data we find ΔH°_f = -25 ± 13 kcal/mole of AlBeO(g).

Aluminum trifluoride vaporizes with a third-law heat ΔH_{298} = 72.7 ± 0.1 kcal/mole AlF_3 and second-law heat ΔH°_{298} = 71.1 kcal/mole AlF_3. AlF is formed from AlF_3 + Al with $\Delta H^\circ_v 298$ = 56.0 ± 0.2 kcal/mole AlF and $\Delta H^\circ_f 298$ = -63.3 ± 0.7 kcal/mole AlF.

A preliminary value for the heat of formation of $AlBF_4$ was found, $\Delta H^\circ_f 298$ = -396 kcal/mole of $AlBF_4(g)$.

1. INTRODUCTION

During the past three years thermodynamic data have been obtained on condensed and vapor systems by measuring pressures using Langmuir and Knudsen techniques. The procedures have involved the use of vacuum balance equipment and a high temperature mass spectrometer. The mass spectrometric work was done on Contract No. DA-19-020-5584 in conjunction with A. Büchler and J. L. Stauffer. The elements, compounds and mixed systems studied were B_2O_3, SiO_2, Be-B-O, Al-B-O, Re, BeO, Al_2O_3, Al-Be-O, AlF_3 and AlF. In addition to these pressure measurements, data has been secured on the evaporation coefficients of $B_2O_3(\ell)$, $SiO_2(\ell)$ and $Al_2O_3(\ell)$. The results of these studies are described in this final report.

2. APPARATUS

The apparatus for the vapor pressure measurements consisted of three vacuum balance systems and a high temperature mass spectrometer. Each balance system had its own automatic balance and furnace control.

Two of the balance systems used radiant heating. A "Pyrex" system was limited to about 1100°C by its mullite furnace tube, and a stainless steel system with a platinum-rhodium furnace had an upper temperature limit of about 1600°C. Both systems were designed to be operated under vacuum or pressure. The operating temperature for the stainless steel system using an induction furnace was limited only by the melting point of the container materials.

The mass spectrometer may be operated in excess of 2500°C.

2.1 Vacuum Balance

The rate of effusion or evaporation is detected by continuously measuring the change in weight of a Knudsen cell or target suspended from an automatic-recording microbalance. The balance consists of a quartz truss beam supported vertically at the fulcrum by fine quartz fibers. The hang downs at the end of each arm are also quartz fibers sealed directly to the beam and to quartz hooks.

The balance is held at its null position automatically by an electromagnet acting on a magnet rod suspended from one arm of the balance. The null position is detected with a variable permeance transducer which surrounds a steel rod hanging below the magnet rod. When the balance is displaced from its null a signal is generated by the transducer controller which drives a potentiometer through a servo mechanism. The potentiometer changes the current flowing in the electromagnet, restoring the balance to its null. The current, which is proportional to the weight change, is recorded continuously. The electronic system was patterned after that of Cochran.[1]

2.2 Vacuum Systems

The two stainless systems were designed to achieve pressures in the ultra-high vacuum range 10^{-7} - 10^{-8} torr at temperature. Each has a consolidated PMCU 721 diffusion pump, a foreline trap, and a 5 cubic ft/min mechanical pump.

Both systems are built inside a large degassing oven capable of reaching a temperature of 500°C. The vacuum system is made of stainless steel, "Pyrex" glass and kovar. All joints are sealed with metal gaskets of gold or copper. Both the electromagnet and the transducer mentioned above are mounted outside the balance so that they may be removed during bakeout.

The "Pyrex" system is pumped with a 100 ℓ diffusion pump, foreline trap and mechanical pump. The valves and joints are sealed with greaseless "Viton" O-rings. Pressures in this system were 10^{-6} - 10^{-7} torr. All three systems use Dow 705 pump oil having a vapor pressure at 25° of 3×10^{-10} torr.

2.3 Furnace and Controls

2.3.1 Platinum-rhodium furnace

The apparatus (Fig. 1) consists of a water cooled stainless tube in which is placed a 10-inch long resistance-heated platinum-40% rhodium tube furnace with three platinum radiation shields. The furnace ends are platinum flanges clamped between water-cooled nickel flanges. The electrical leads are water-cooled tubing brazed into the furnace wall at one end. Leads at the other end are electrically insulated by Varian high current feedthroughs which have been drilled for water cooling. Thermocouple leads are brought through a glass press-seal. The platinum-10% rhodium-platinum control thermocouple is welded to the center of the platinum-40% rhodium furnace tube. The leads are insulated with sapphire tubes. This furnace is capable of 1600°C.

Since the thermocouple is 1 to 2 volts ac about ground, a filter of chokes and capacitors was used to avoid swamping the recorder-controller.

The furnace is powered with a saturable reactor controlled by a Leeds & Northrup recorder-controller connected to the platinum-10% rhodium-platinum thermocouple. Temperature is maintained to better than ± 1/2°C.

2.3.2 Induction Furnace

This equipment is shown in Fig. 2. An internal work coil is brought into the water-cooled stainless furnace with a Varian r.f.

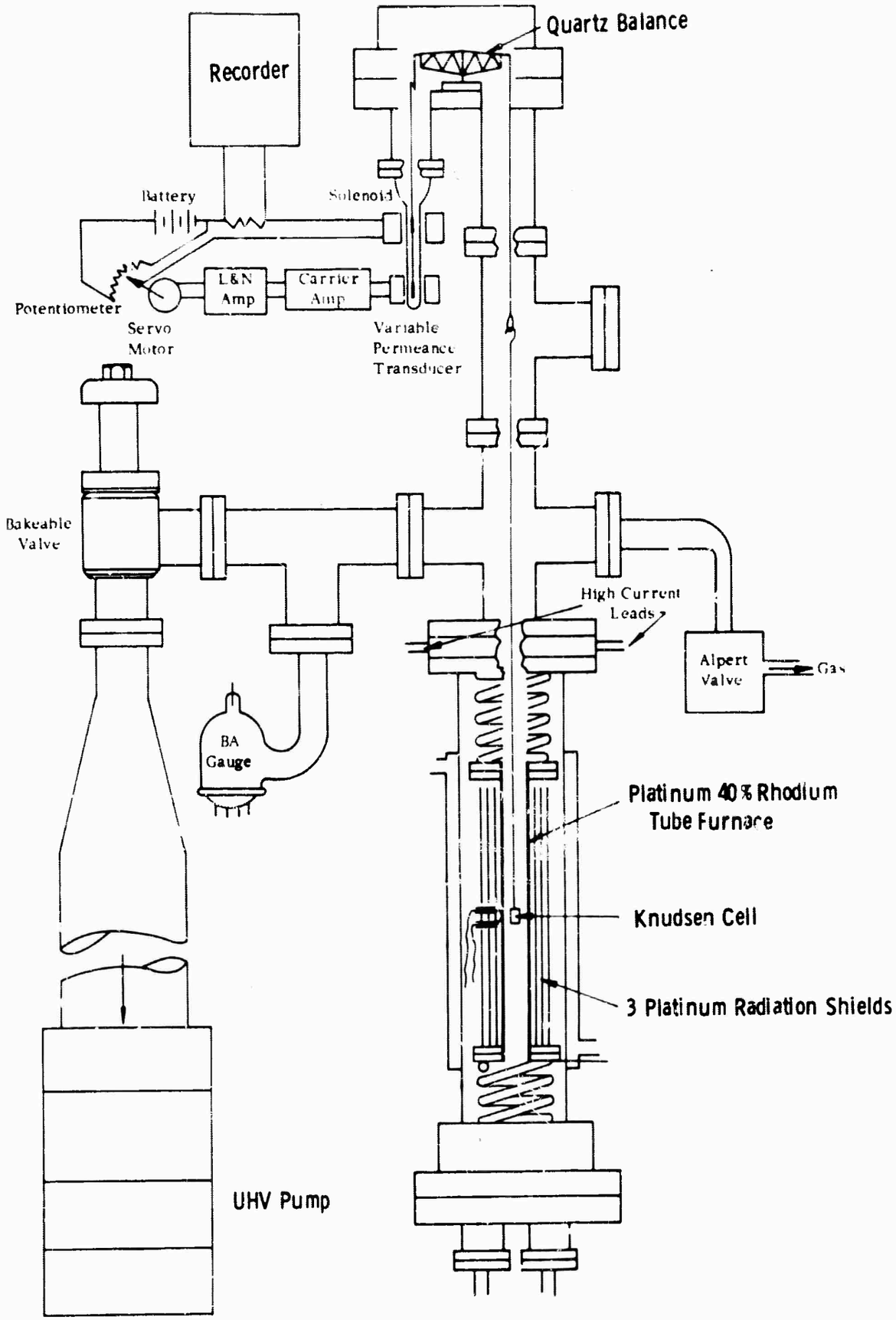

FIGURE 1 HIGH VACUUM MICROBALANCE SYSTEM

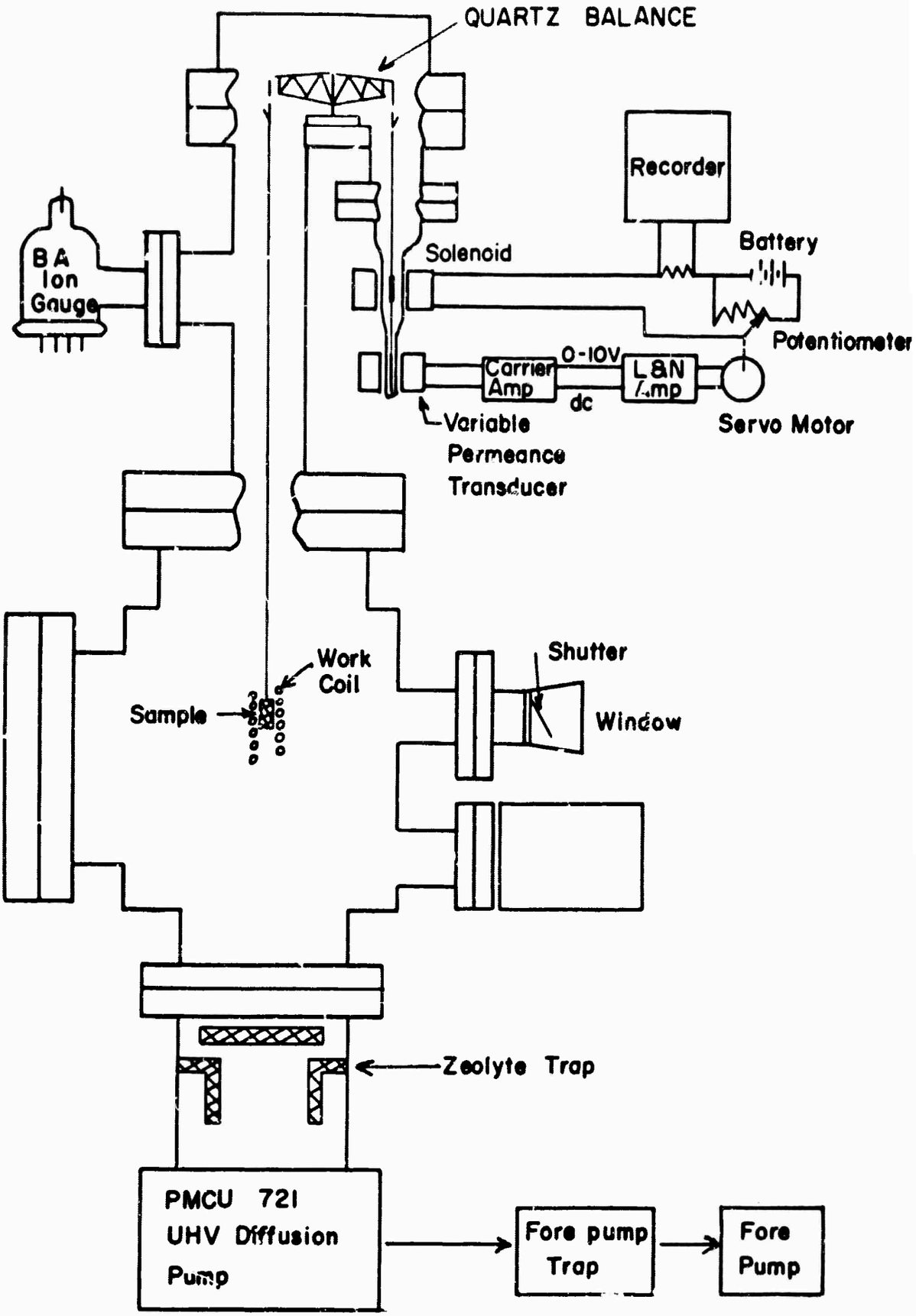

FIGURE 2 VACUUM MICROBALANCE, INDUCTION FURNACE AND PUMPING SYSTEM

feedthrough. Power from the Westinghouse 20 kw induction furnace is maintained constant with a saturable reactor. The latter is governed by a Leeds & Northrup controller fed by a rectified attenuated voltage from a torroidal pickup coil on one of the r.f. leads. Although the magnetic field in or above the work coil produces an apparent weight change at different induction power outputs, there is no significant change in apparent weight with time while the power is controlled at a fixed output. Confirmation of good power control is found in optical pyrometer temperature readings which may vary no more than ± 2°.

2.3.3 Pyrex system

A bifiliarly wound resistance furnace heats the mullite tube furnace in the third system. Temperatures are controlled with a West proportional controller and saturable reactor.

2.4 Mass Spectrometer

The high temperature mass spectrometer is a 12"-radius, 60° sector, magnetic deflection instrument manufactured by Nuclide Corporation. Before the present research, extensive tests were carried out with silver and B_2O_3 to establish the conditions necessary for obtaining precise second-law heats of vaporization. It was found that placing the thermocouple at the base of a Knudsen cell which was inside a thick-walled molybdenum crucible yielded quite reproducible slopes (Fig. 3). In this position the thermocouple measured the temperature of the vaporizing material, which was held at the bottom of the cell.

3. SAMPLES

Boric oxide from the U.S. Borax Corp. contained 4.5% H_2O which was removed by heating in vacuum. 99.97% silica rod was obtained from General Electric. The BeO from Nuclear Metals had no significant impurities. Al_2O_3 powder from A.D. MacKay was better than 99.9% pure.

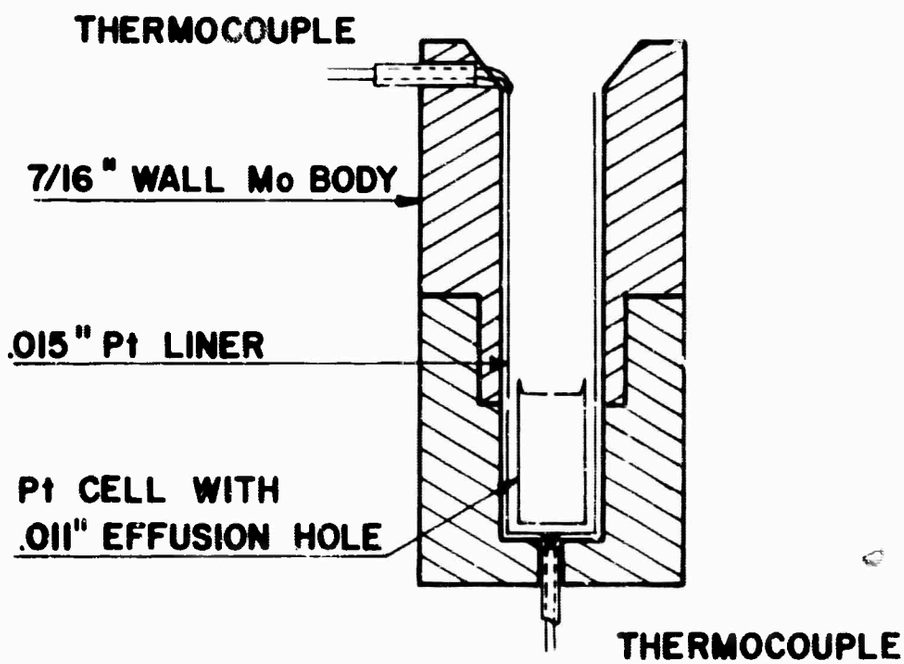

FIGURE 3 MOLYBDENUM-PLATINUM CRUCIBLE

$Al_4B_2O_9$ and $Al_{18}B_4O_{33}$ were prepared at Philco Aeronutronics and were very kindly furnished by Dr. D. L. Hildenbrand. Each sample contained 2 to 5% excess Al_2O_3. Rhenium obtained from the Rembar Co. was 99.97% pure. Principal impurities were in ppm: Fe, 70; Mo, 25; C, 20; N, 10; and O, 40. Sapphire rod was secured from Linde Company. The AlF_3 from Matheson, Coleman and Bell had some volatile impurities, probably water, which were removed by heating under vacuum. Aluminum powder was filed from a pure single crystal.

4. PROCEDURE

In all three systems, filled Knudsen cells weighing less than 1 gram were suspended from the balance. A cell made of rhenium was too heavy to hang from the quartz beam so a target was suspended instead. Vapor pressures were measured by comparing the fraction of vapor sticking to the target to that evaporating from the cell. To do this both target and cell were measured before and after each series of experiments. Targets were glass cover slides held in quartz frames.

5. RESULTS AND DISCUSSION

5.1 B_2O_3 Vapor Pressure and Evaporation Coefficient

Since this compound has been studied by a number of investigators, it appeared to be a good substance on which to test the apparatus. Moreover, our tests would also establish a baseline for the later study of other systems involving B_2O_3.

Although the spread in the pressures found is not unusually great, the second-law slopes vary from 77 to 93 kcal. The early and long accepted measurements on B_2O_3 were made by Speiser et al.[2] Subsequent investigators have suggested that Speiser's results may have been in error because of water adsorption during the intermittent weighings. This would lead to relatively higher weight losses for low temperature measurements and thus to a lower slope. However, the excellent agreement between the weight loss and target gain in his

measurements would appear to be inconsistent with this hypothesis. Furthermore, some experiments undertaken by us on the rate of adsorption of water by large pieces of glassy B_2O_3 indicate that this reaction is too slow to account for the low slopes.

It seems more likely that if errors were present in Speiser's data, it was in temperature measurement. An inductively heated thin wall cell has a radial thermal gradient which is a function of the cell diameter, wall thickness and temperature. Samples supported from the bottom will also have vertical gradients depending on the coil configuration, support rod size and position of cell within the coil. A combination of these factors would favor a positive error throughout the temperature range with the greatest error at the upper end of the scale. This error is most prominent with relatively large diameter cells and for cells in which the orifice serves as a blackbody. Gradients will be greater at higher temperatures as well. Temperature measured in the orifice will be weighted toward the higher temperatures, since the radiant flux is proportional to T^4. Thus measurements taken in the orifice give no assurance of freedom from error. Three possible remedies for this situation are (1) the use of small diameter cells, (2) confining the volume of the cell within a larger thick-walled crucible, (3) radiant heating with susceptors. It is interesting to note that the most recent experiments, whose measurements give the highest slopes, have used the second solution (with thermocouple) and the third solution (with optical pyrometer).[3,4]

The foregoing discussion also applies to electron bombarded cells, although the customary radiation shields may reduce the error. The measurements in this research have been made with 1/4" dia. cells heated radiantly. Temperature was determined by calibrating the furnace with a thermocouple placed inside.

B_2O_3 pressures were measured here to establish that the apparatus was working properly and to construct a baseline for this compound on our equipment and using our techniques. While some equipment faults were discovered and corrected, it was also found that B_2O_3 has a low evaporation coefficient not previously reported. Evaporation coefficient measurements were made in two ways: (1) by comparing Knudsen and Langmuir measurements, and (2) by varying the orifice size and applying the Motzfeldt[5] equation.

In the B_2O_3 Langmuir experiments an open 1/4" diameter platinum bucket was filled with B_2O_3 and the evaporation rate measured with the vacuum balance. In both the Langmuir and the second set of Knudsen measurements the liquid B_2O_3 formed a meniscus whose area was calculated by assuming it had a parabolic shape. Effusion rates were determined by using a very small orifice, i.e. 2.5×10^{-4} cm^2 corrected for the Clausing factor. The data are given in Table I and a Van't Hoff plot is shown in Fig. 4. From the different pressures P_L and P_K, where L refers to Langmuir and K to Knudsen, we calculate

$$\alpha_e = P_L/P_K = 0.03 \pm .01 \qquad (1)$$

TABLE I

BORIC OXIDE VAPOR PRESSURE

Langmuir Experiments

T,°K	Time, sec	Weight Loss, μg	Evap.[a] rate $g\text{-}cm^{-2}\text{-}sec^{-1} \times 10^9$	Press.[b] atm $\times 10^{10}$
1201	25,200	48	3.89	3.64
1201	77,400	138	3.64	3.41
1359	2,304	400	355.	353.
1391	1,059	400	772.	777.
1422	443	400	1850.	1850.
1459	200	400	4090.	4210.

a. Area = 4.89×10^{-1} cm^2

b. Calculated from free evaporation - non-equilibrium pressure

Knudsen Experiments

T, °K	Time sec	Weight Loss µg	Evap. rate[c] $g\text{-}cm^{-2}\text{-}sec^{-1} \times 10^{6}$	Press. atm. $\times 10^{7}$	Δfef[d] cal/deg	Heat of Vaporization ΔH°_{298} kcal/mole
1297	50,400	40	3.16	3.08	46.29	98.7
1328	60,000	100	6.64	6.54	46.20	98.9
1422	4,800	72	59.8	61.0	45.84	99.1
1459	2,400	68	113.0	117.0	45.11	99.6
1502	6,600	420	254.0	266.0	45.55	99.9
					Avg. =	99.2 ± 0.4

c. Orifice area corrected for Clausing factor = 2.51×10^{-4} cm^2
d. JANAF, December 1964.

The effect of water vapor on the evaporation was particularly noticeable in the Langmuir study, where a large amount of B_2O_3 was used. This resulted in high initial evaporation rates and rejection of early Langmuir measurements.

A least squares fit to both Langmuir and Knudsen measurements gives a common slope of ΔH_{1350} 92.6 ± 1.6 kcal/mole, in excellent agreement with Hildenbrand, et al.[4] and Büchler, et al.[3] who found 93.3 and and 93.6 ± 3 kcal/mole, respectively. A third-law heat of vaporization ΔH°_{298} is 99.2 ± 0.4 kcal/mole for Knudsen measurements. The orifice to sample area for this cell is so small that the measured pressure should be only 1% less than the calculated equilibrium pressure.

Our second and third-law heats may be compared in Table II.

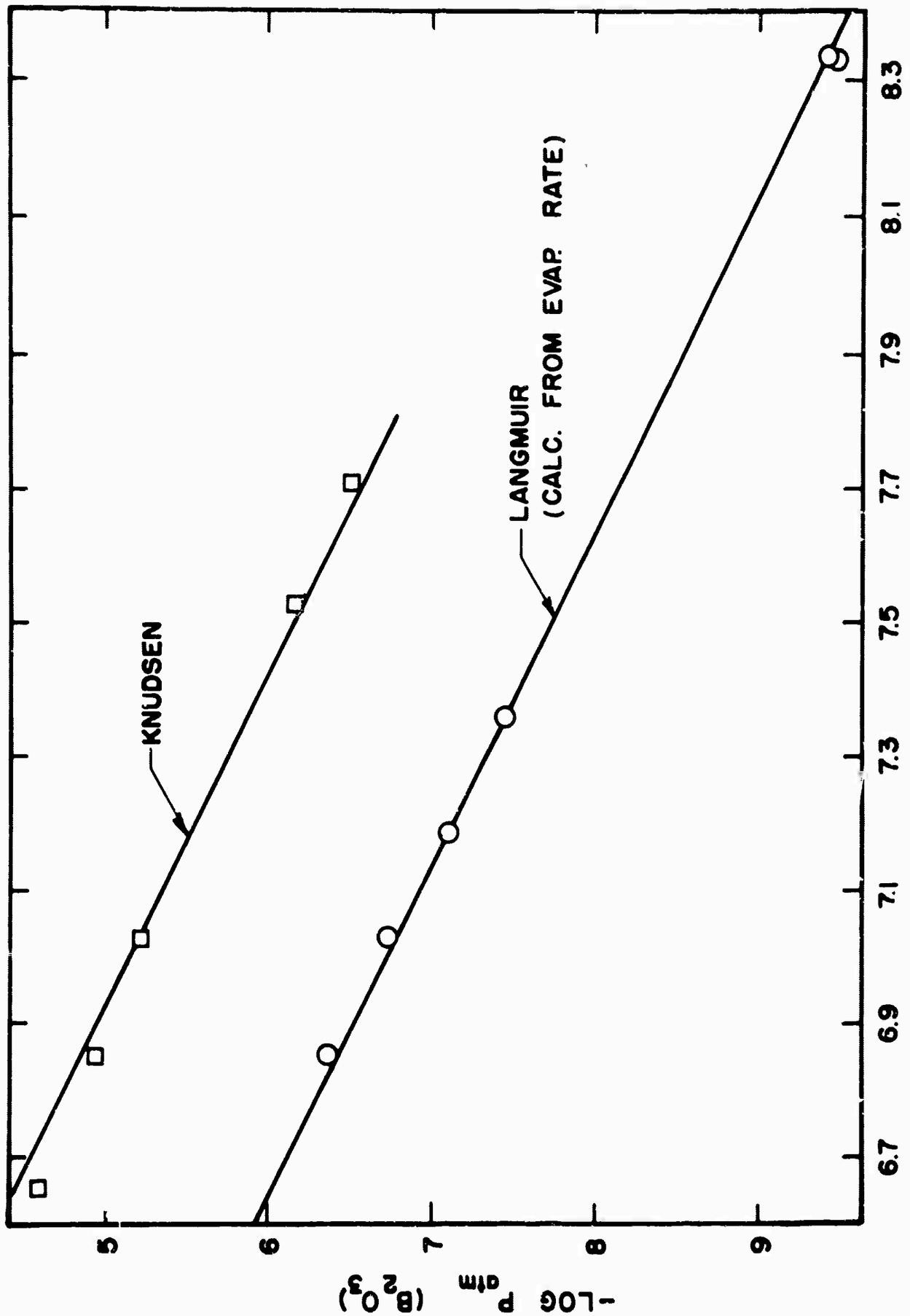

FIGURE 4 COMPARISON OF KNUDSEN AND LANGMUIR VAPORIZATION OF B_2O_3

TABLE II

Heat of Vaporization of B_2O_3

	Range	$\Delta H_V 298$ Third Law	$\Delta H_V 298$ Second Law	$\Delta H_f^\circ 298$
May 1963	1325-1547	99.4 ± 0.2*	92.8 ± 1.4*	-199.9
May 1965	1201-1502	99.2 ± 0.4*	99.6 ± 1.6**	-200.1
Average of nine measurements in JANAF[10] excluding that of Cole and Taylor		99.5 ± 0.8	90.7 ± 8.2	-199.6 ± 0.8

* Knudsen measurements only
** Knudsen and Langmuir measurements

In the Motzfeldt treatment, the platinum Knudsen cells were one-quarter inch in diameter and three-eighths inch high. A tight fitting removable top permitted changing the orifice area. Measurements were made at several temperatures and were normalized to 1391°K to compute the evaporation coefficient. For this calculation, a heat of vaporization of 92.6 kcal/mole was used. The data are presented in Table III.

TABLE III

Evaporation Coefficient of $B_2O_3(\ell)$ by Motzfeldt Method

T, °K	$\frac{aW_a}{B} \times 10^2$	P_m atm $\times 10^7$	P_m atm $\times 10^6$ normalized to 1391°K	$\alpha_e \times 10^2$
1422	3.19	37.2	1.71	5.9
1391	3.19	18.4	1.84	8.7
1359	3.19	8.18	1.80	7.7
1359	12.9	3.95	0.87	4.4
1391	12.9	10.1	1.01	5.7
			Avg.	$6.4 \pm 2 \times 10^{-2}$

The evaporation coefficient was computed from Motzfeldt's[5] equation,

$$P_m = P_{eq} - \frac{aW_a}{B}\left(\frac{1}{\alpha_e} + \frac{1}{W_B} - 2\right) P_m \qquad (2)$$

which may be rearranged with $1/W_B - 2 \approx 0$, to

$$\alpha_e = \frac{aW_a}{B}\left(\frac{P_m}{P_{eq} - P_m}\right) = 6 \pm 2 \times 10^{-2} \qquad (3)$$

where a is the orifice area; W_a, its Clausing factor; B, the sample area; P_m, the measured pressure and P_{eq}, the equilibrium pressure. P_m is found by using Langmuir's equation and the measured effusion rate. P_{eq} (2.34×10^{-6} atm at 1391°K) was taken from the data given in Table I, where aW_a was 2.5×10^{-4} cm^2 and aW_a/B was 4.5×10^{-4}. Two measurements in which $aW_a/B = 1.13 \times 10^{-2}$ were not included in Table III. The measured pressures were too close to equilibrium to give meaningful values for α_e, considering the scatter in the data. In order to measure an evaporation coefficient of this magnitude (0.06) by the Motzfeldt method, it is necessary to use relatively large orifice to sample area ratios.

Within the precision of the present data, the Motzfeldt equation appears to give satisfactory results for $B_2O_3(\ell)$. These data cannot be considered a test of Rosenblatt's[6] criticism of Motzfeldt's equation.

Rosenblatt suggests that the evaporation coefficient may be a function of the degree of vapor saturation over the condensed phase. In the case of liquids, however, Hirth and Pound[7] state that the evaporation coefficient and condensation coefficient should be equal.

It has been pointed out by Wyllie,[8] Mortensen and Eyring,[9] and by Hirth and Pound[7] that polar molecules which are associated in the liquid state should have a low condensation coefficient. The impinging molecule must be properly oriented with respect to the liquid molecules in order to be integrated into the liquid phase. Otherwise the molecule will "bounce" from the surface of the liquid. Three examples of polar liquids are methyl, ethyl alcohol, and water. These three are associated in the liquid state by hydrogen bonds and have condensation coefficients of 0.02 to 0.05.[7] B_2O_3, with a similar condensation coefficient, is thought to form a network structure in the liquid phase, with single bonds from each boron atom to three surrounding oxygen atoms. Thus the evaporation coefficient of about 0.04 for B_2O_3 is reasonable when compared to other associated liquids.

5.2 SiO_2 Vapor Pressure and Evaporation Coefficient

Another high temperature associated liquid is SiO_2. It vaporizes as predominately $SiO + 1/2\ O_2$, with a small percentage of SiO_2 in the vapor.

Several investigators have measured the heat of formation of SiO(g) by reducing SiO_2 with either Si or H_2. Only two sets of vapor pressure measurements have been made on SiO_2 under neutral conditions. Brewer and Nastick[11] made three measurements between 1840 and 1951°K using a platinum cell. Their tests yielded $\Delta H_f 298 = -30 \pm 4$ kcal/mole SiO(g). Porter, Chupka and Inghram[12] measured SiO_2 in an alumina lined cell. Their measurements give $\Delta H^\circ_f 298 = -40 \pm .5$ kcal/mole SiO(g). Both measurements are more exothermic than those made under reducing conditions. No one has measured the evaporation coefficient of SiO_2.

Quartz was heated in a rhenium Knudsen cell and the vapor condensed on a target suspended from a vacuum balance. The rhenium cell, the vapor pressure of which is given later in this report, had an orifice in a removable lid and a hole drilled in its side for

measuring temperature. All measurements were made above the melting point of quartz. Six measurements were made with the lid on and five with an open cell. In the first three Knudsen measurements there was a decrease in effusion rate with time, presumably because the sample was losing water. The Knudsen measurements are given in Table IV together with a third-law heat for the reaction

$$SiO_2(\ell) = SiO(g) + 1/2\ O_2 \qquad (4)$$

From the Knudsen measurements a heat of formation for SiO(g) is calculated as $\Delta H^\circ_f 298 = -22.6 \pm 1.0$ kcal/mole. This is in good agreement with the value in the latest JANAF Tables[10] (-24.2± 1 kcal) based on the formation of SiO under reducing conditions. These data are used to construct a curve (Fig. 5) for effusion rates corrected for the evaporation coefficient described below.

TABLE IV

Pressure of SiO over Liquid SiO_2

T,°K	t sec x 10^{-3}	Target gain µg	Total[a] Evap. Rate	Evap.[b] rate SiO g-cm^{-2}-sec^{-1} x 10^5	P[c] atm x 10^5
1993	2.40	30	4.94	3.40	1.09
2053	3.60	88	9.65	6.59	2.13
2095	2.40	92	15.1	10.3	3.36
2146	6.60	410	24.5	16.6	5.48
2198	3.00	400	52.7	35.5	11.9
2032	4.20	55	5.17	3.54	1.14

a. Top orifice area = 1.14 x 10^{-2} cm^2; fraction striking target = 0.0222

b. Using calculated ratios for SiO(g) and SiO_2(g) from JANAF

c. Extrapolated to zero orifice size, i.e. 2.14 P_m

Heat of formation of SiO(g)

T, °K	$-R\ln P_{SiO}$ cal/deg	$-1/2\ R\ln P_{O_2}$ cal/deg	$-\Delta fef^{d}$ cal/deg	$\Delta H°_{r}298^{e}$ kcal	$-\Delta H°_{f}298^{f}$ kcal
1993	22.71	12.21	60.93	191.0	24.9
2053	21.38	11.53	60.82	192.4	23.5
2095	20.47	11.08	60.73	193.3	22.6
2146	19.50	10.60	60.63	194.7	21.3
2198	17.80	9.75	60.53	193.6	22.3
2032	22.62	12.16	60.86	194.3	21.6
				Avg.	-22.6 ± 1.0

d. JANAF Tables

e. Heat of reaction for $SiO_2(\ell) \rightarrow SiO(g) + 1/2\ O_2$

f. Heat of formation of SiO(g) with $\Delta H_f 298\ SiO_2(\ell) = 215.9$ kcal

The open cell evaporation rates are given in Table V and plotted in Fig. 5. The ratio of Langmuir (open cell) and corrected Knudsen measurements,

$$P_L/P_K \qquad \alpha_e = 5 \times 10^{-3} \tag{5}$$

gives the evaporation coefficient. This value is about one-tenth that found for B_2O_3. If the low evaporation coefficient is due to restricted rotation arising from bonding in the liquid as suggested by Kincaid and Eyring,[13] the lower evaporation coefficient for SiO_2 may be caused by its three dimensional bonding compared to B_2O_3 which is bonded two-dimensionally.

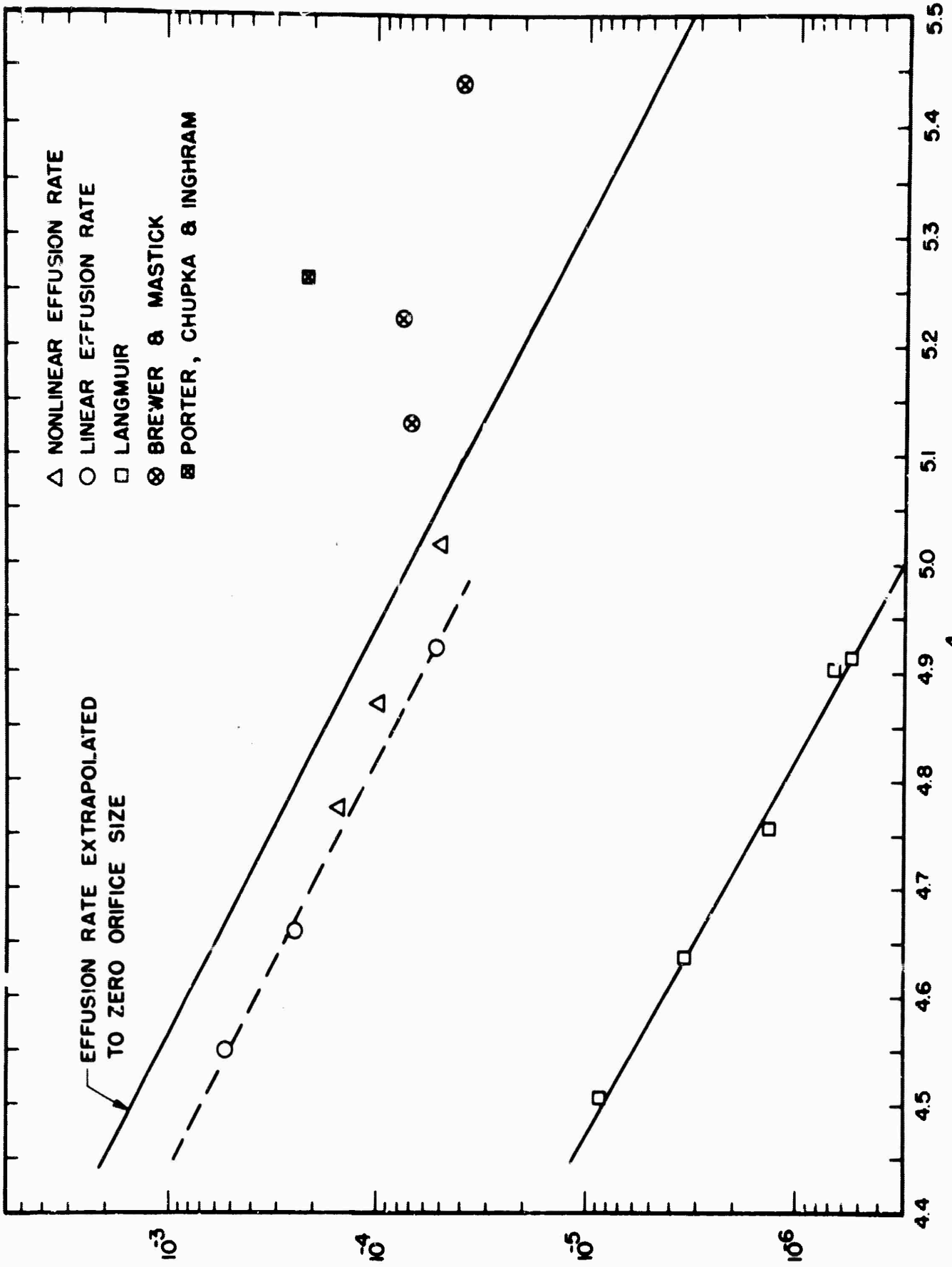

FIGURE 5 EFFUSION AND EVAPORATION RATES OF SiO_2 (1)

TABLE V

Evaporation Rate of SiO_2 from Open Rhenium Crucible

T, °K	t sec	Target gain μg	Evaporation rate $g\text{-}cm^{-2}\text{-}sec^{-1} \times 10^7$
2035	5400	71	5.17
2101	4800	160	13.1
2157	1800	154	33.6
2218	5400	1180	85.8
2039	1800	30	6.55

Fraction striking target = 0.0264

Area = 0.965 cm^2

5.3 Be-B-O System

Until the present study of the Be-B-O system, only one compound, $Be_3B_2O_6$, had been identified by X-ray,[14,15] and no phase diagram or thermodynamic data were available. A vacuum balance, differential thermal analysis and mass spectrometry were used in our research to establish the phase diagram and thermodynamics.

5.3.1 Microbalance Measurements

Vapor pressure as a function of composition in the $BeO\text{-}B_2O_3$ system was obtained by determining the rate of effusion from a Knudsen cell whose weight change was continuously measured. The first weight change measurements were made in the temperature range between 1080° and 1250°C, with orifice areas between 2.3×10^{-3} and 1.8×10^{-2} cm^2. These data indicated the existence of a two-phase region extending from $B_2O_3(\ell)$ to at least 50 mole percent BeO, as manifested by a constant pressure equal to that of $B_2O_3(\ell)$. The existence of at least one compound was revealed, for the pressure decreased in the range from 50 to 70 mole percent BeO. In none of these measurements, however, was equilibrium established after the pressure dropped. This is

evidenced by the lack of constant pressure regions corresponding to other two-phase domains. To obtain consistent results, as shown by well-defined two-phase areas, it was necessary to use very small orifices. Two separate measurements were made, one at 1562°K with an orifice area of 5.5×10^{-4} cm^2, a second at 1398°K with an orifice area of 1.4×10^{-3} cm^2. The larger orifice was necessary at the lower temperature because of time limitations. Even with an orifice of this size, the measurement required three weeks.

The results of the two experiments are shown in Fig. 6, in which the logarithm of the B_2O_3 activity with $B_2O_3(\ell)$ as standard state is plotted against composition. The data of Fig. 6 indicate that the compound $Be_3B_2O_6$ identified earlier by low temperature X-ray studies,[14,15] is in fact the only stable intermediate phase in this system. The drop-off in B_2O_3 activity as the 75% composition is approached is typical of a phase change in binary systems.[16,17] A drop-off in activity as pure BeO is approached may be due to a decrease in effective evaporating surface through formation of BeO and to a low evaporation coefficient for the vaporization of B_2O_3 from $Be_3B_2O_6$.

5.3.2 Differential Thermal Analysis Measurements

To construct a phase diagram for the BeO-B_2O_3 system consistent with the vaporization data, it was necessary to establish the melting point of the compound $Be_3B_2O_6$. The liquidus in the neighborhood of this compound was found by differential thermal analysis. In this procedure, the difference in temperature between a sealed capsule containing a mixture of BeO and B_2O_3 in the ratio $3BeO:1.15B_2O_3$ and a second capsule containing aluminum oxide was measured during cooling. The two capsules, placed side by side, were heated in a globar tube furnace. Platinum-platinum 10% rhodium thermocouples inserted in wells inside each capsule were used to measure temperature. One recorder was used to indicate the temperature of the capsule containing the experimental mixture, while a second recorder was used for the

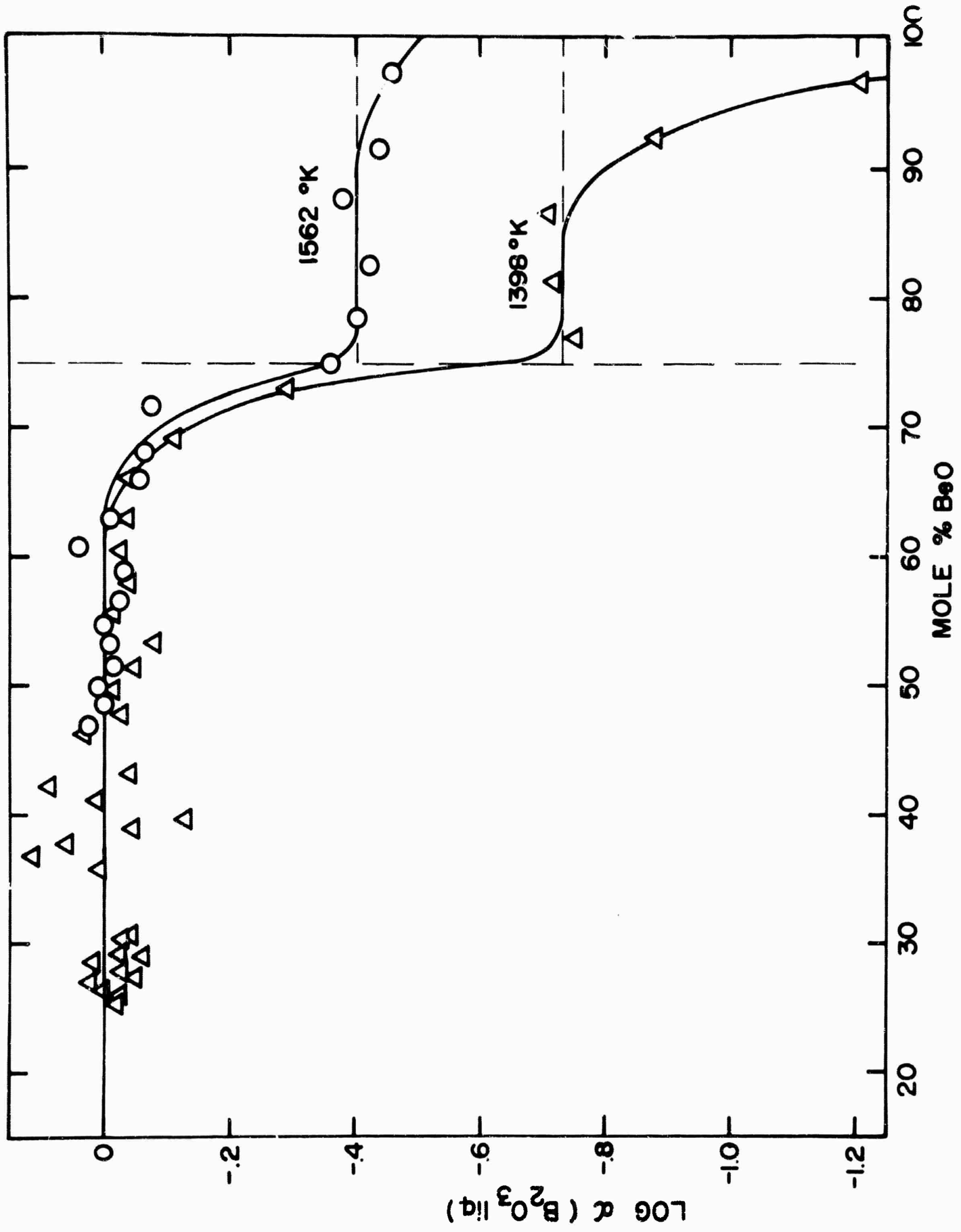
1562 °K
1398 °K
LOG α (B_2O_3 liq)
0
-.2
-.4
-.6
-.8
-1.0
-1.2
20
30
40
50
60
70
80
90
100
MOLE % BeO

temperature difference between the two capsules. Three inflections were observed: (1) the point at which freezing started, 1488°C; (2) the temperature where freezing ceased, i.e. the eutectic temperature, 1441°C; (3) the point where the cooling differential between the two capsules was re-established. No other inflections were observed in the differential curve, indicating the absence of other phases stable at lower temperatures. Our data yields a melting point for the stoichiometric compound $Be_3B_2O_6$ of 149[illegible] ± 5°C. Thus, all vapor pressure measurements were made over solid $Be_3B_2O_6$ and either BeO(c) or $B_2O_3(\ell)$. On the basis of the data a phase diagram of the B_2O_3-BeO system can be drawn as shown in Fig. 7.

5.3.3 Mass Spectrometric Studies

Mass spectrometric samples were prepared in our laboratories. To obtain the mixed oxide $Be_3B_2O_6$, a mixture of BeO and B_2O_3 powders was reacted in sealed platinum capsules at 1300°C for 100 hours.

Four series of mass spectrometric measurements were made, three over the two phase region $B_2O_3(\ell)$ + $Be_3B_2O_6$(c) and one over the two-phase region $Be_3B_2O_6$(c) + BeO(c). In each case, the principal ionic species observed was $B_2O_3^+$, corresponding to the neutral boron oxide B_2O_3(g). The principal beryllium-containing ionic species was $Be(BO_2)_2^+$, corresponding to neutral beryllium metaborate $Be(BO_2)_2$(g).

The three measurements on the sample containing excess B_2O_3 yielded results apparently unaffected by the quantity of sample material or the cell orifice areas. Two of these measurements were made with nickel cells of the design described elsewhere,[3] one containing about 5 mg each of BeO and B_2O_3 and one containing 26 mg B_2O_3 and 10 mg $Be_3B_2O_6$. Both cells had orifices of 7.8×10^{-3} cm^2. In the third experiment the crucible design of Fig. 3 was used with the platinum cell having an orifice area of 4.8×10^{-4} cm^2. The results of the three experiments were combined to give the data shown in Fig. 8,

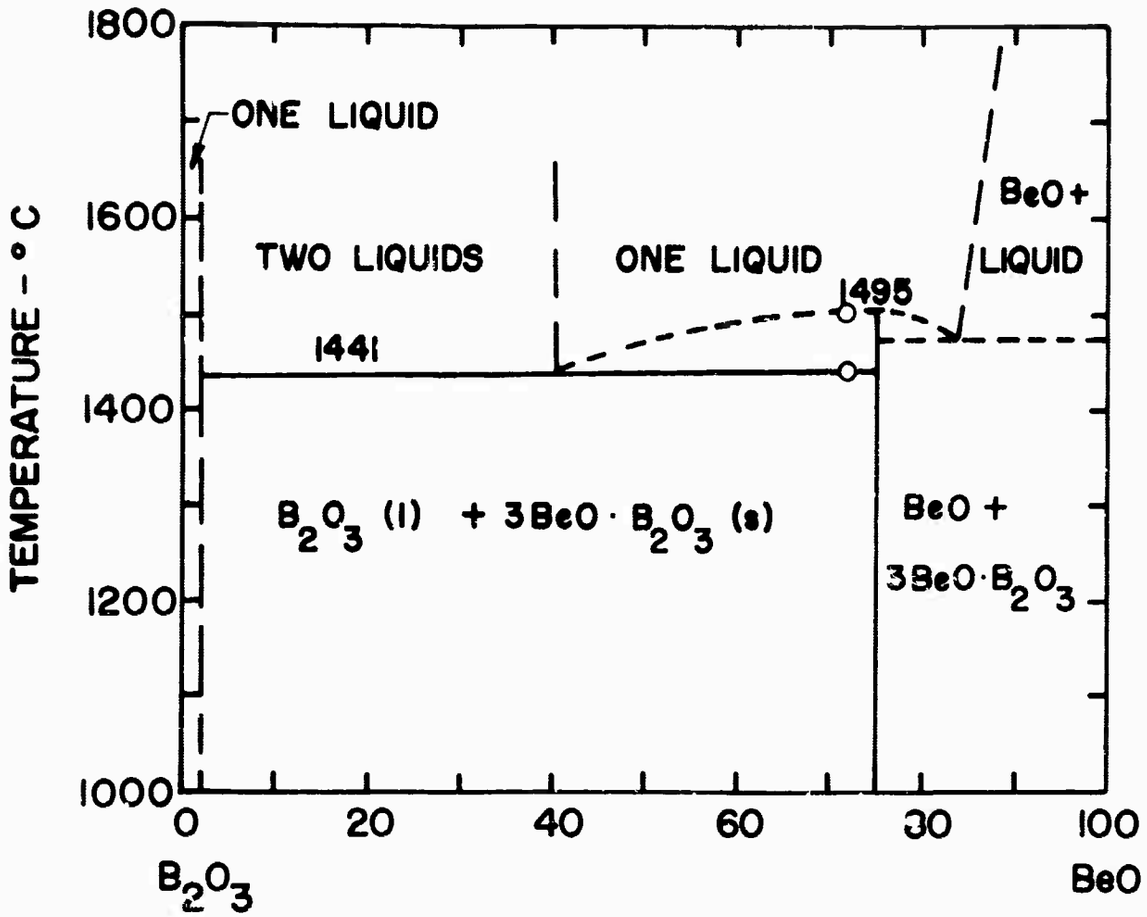

FIGURE 7 B_2O_3-BeO PHASE DIAGRAM

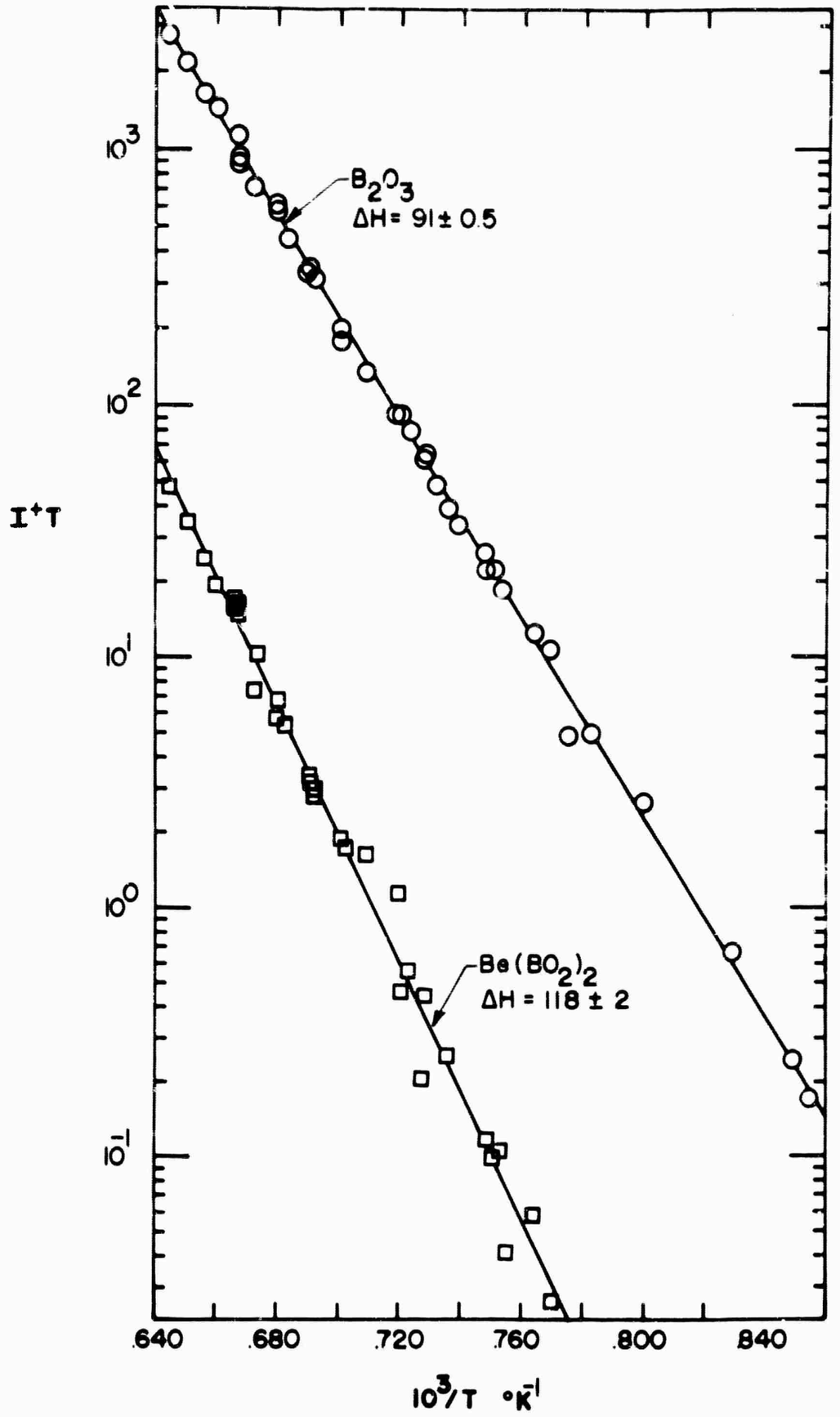

FIGURE 8 PLOTS OF I^+T vs 1/T FOR VAPORIZATION OF $B_2O_3(g)$ AND $Be(BO_2)_2(g)$ FROM THE SYSTEM $Be_3B_2O_6(c)$-$B_2O_3(\ell)$

which gives the temperature dependence of the $B_2O_3^+$ and $Be(BO_2)_2^+$ ion intensities. The second-law heat of vaporization for B_2O_3 found from these experiments is 91 kcal/mole, in good agreement with 93 ± 3 kcal/mole obtained in earlier experiments.

To obtain data for the BeO-rich side of the diagram a platinum-lined molybdenum crucible containing 68 mg of $Be_3B_2O_6$ and 12 mg of BeO was used. It had an orifice area of 4.8×10^{-4} cm^2. The data obtained for both B_2O_3 and beryllium metaborate gas are shown in Fig. 9.

The second-law heats indicated on Figs. 8 and 9, found by a least squares fit of the data, correspond to the following reactions:

(a) $B_2O_3(\ell)$-$Be_3B_2O_6(c)$ (Fig. 8)

$$B_2O_3(\ell) \rightarrow B_2O_3(g) \quad \Delta H_1 = 91 \pm 0.5 \text{ kcal} \tag{6}$$

$$\frac{1}{3} Be_3B_2O_6(c) + \frac{2}{3} B_2O_3(\ell) \rightarrow Be(BO_2)_2(g) \quad \Delta H_2 = 118 \pm 2 \text{ kcal} \tag{7}$$

(b) $Be_3B_2O_6(c)$-BeO(c) (Fig. 9)

$$Be_3B_2O_6(c) \rightarrow 3BeO(c) + B_2O_3(g) \quad \Delta H_3 = 112 \pm 1 \text{ kcal} \tag{8}$$

$$Be_3B_2O_6(c) \rightarrow 2BeO(c) + Be(BO_2)_2(g) \quad \Delta H_4 = 137 \pm 3 \text{ kcal} \tag{9}$$

From these least squares curves, the heats of formation of the condensed phase mixed oxide, $Be_3B_2O_6(c)$, and the gaseous mixed oxide $Be(BO_2)_2(g)$, can be obtained. The heat of reaction for:

$$3BeO(c) + B_2O_3(\ell) \rightarrow Be_3B_2O_6(c) \tag{10}$$

can be obtained from the pairs of reactions (6) and (8), and (7) and (9), and a third value for the heat of this reaction can be obtained

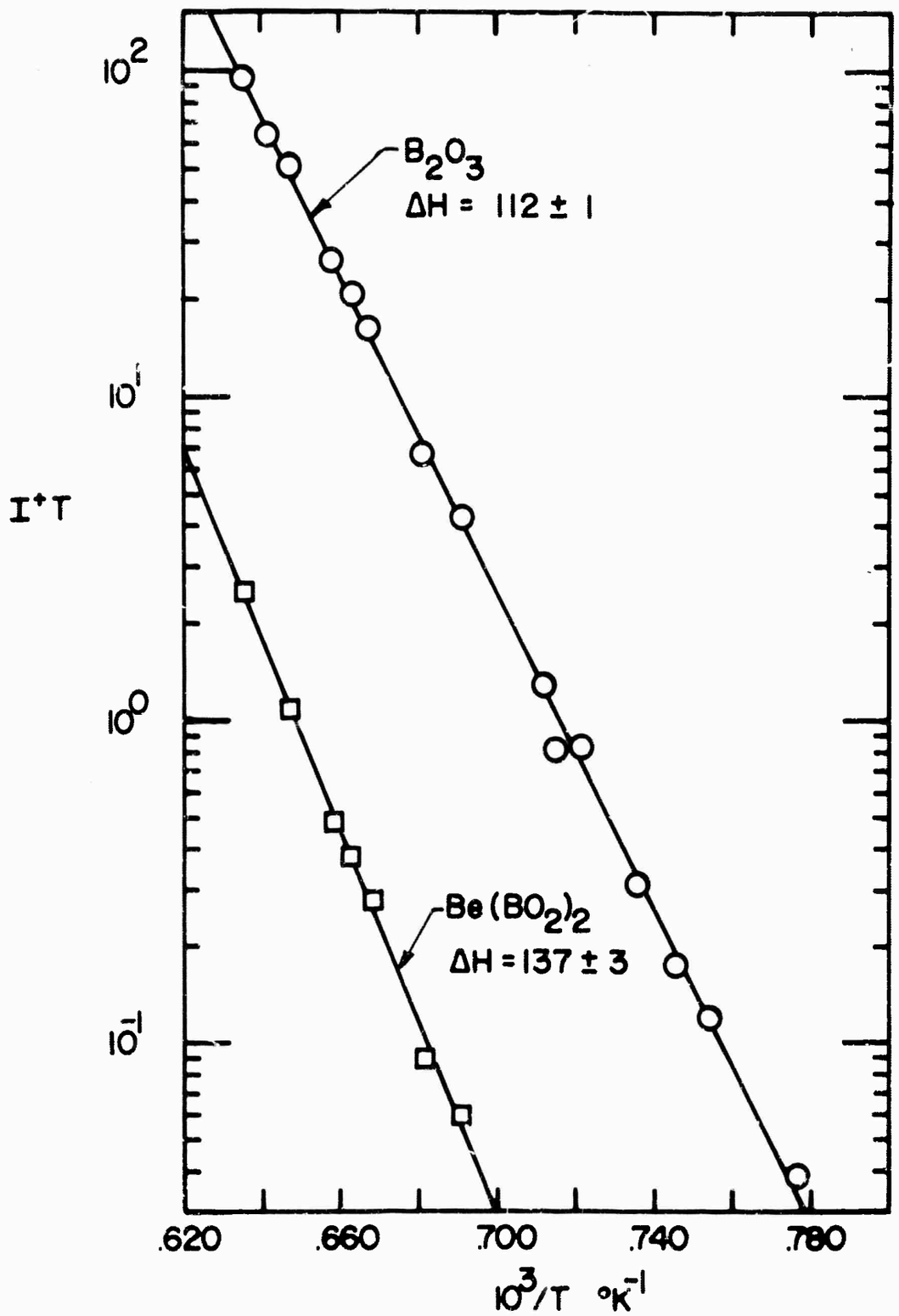

FIGURE 9 PLOTS OF I^+T vs 1/T FOR VAPORIZATION OF $B_2O_3(g)$ and $Be(BO_2)_2(g)$ FROM THE SYSTEM $Be_3B_2O_6(c)$-BeO(c)

from the B_2O_3 activity data obtained in the weight loss experiments. The three values are -21, -28.5 and -20 kcal respectively, which yield a best estimate for reaction (5) of ΔH_{10} = -23 ± 5 kcal/mole. The heat of formation of the gaseous metaborate from the oxides

$$BeO(c) + B_2O_3(g) \rightarrow Be(BO_2)_2(g) \qquad (11)$$

can be obtained from the values above; on the BeO-rich side it is 25 kcal, and on the B_2O_3-rich side it is 19 kcal. From these we find as best estimate for reaction (11) ΔH_{11} = 22 ± 5 kcal/mole.

In order to obtain entropy values consistent with the measured pressures and second-law heats, entropy changes for reactions (6) through (9) were calculated from

$$\Delta S_{1500} = \frac{\Delta H_{1500}}{1500} + R \ln p \qquad (12)$$

where p is the vapor pressure of the gaseous species and ΔH_{1500} is the heat of reaction computed from the values in Table VI. The B_2O_3 pressure at 1500°K given by our vacuum balance data is 2.70×10^{-5} atm. Using this pressure, the ion intensities of $B_2O_3^+$ and $Be(BO_2)_2^+$ from the mass spectrometric data, and Otvos and Stevenson's[18] ionization cross sections, the pressures were computed at 1500°K for reactions (7) through (9). The data taken from platinum cells over the $BeO\text{-}Be_3B_2O_6$ system were normalized to the orifice area and sample-to-ion source distance of the nickel cells.

Using the above procedure, the following pressures (in atmospheres) and entropy changes were calculated for reactions (6) through (9): (6) $p_{B_2O_3} = 2.7 \times 10^{-5}$, ΔS_6 = 39.6 eu; (7) $p_{Be(BO_2)_2} = 2.5 \times 10^{-7}$, ΔS_7 = 50.3 eu; (8) $p_{B_2O_3} = 9.3 \times 10^{-6}$, ΔS_8 = 53.0 eu; (9) $p_{Be(BO_2)_2} = 1.1 \times 10^{-7}$, ΔS_9 = 59.1 eu.

TABLE VI

Thermodynamic Values for Be-B-O System

	$\Delta H_{1500}(f)$ kcal/mole	S°_{1500} eu/mole
$BeO(c)$ [a]	-142.3	19.8
$B_2O_3(\ell)$ [a]	-294.7	61.3
$B_2O_3(g)$ [b]	-204	101
$Be_3B_2O_6(c)$ [b]	-745	108
$Be(BO_2)_2(g)$ [b]	-324	127

a. Reference 10
b. This work

The entropies for reactions (10) and (11) were calculated from the entropy changes for reactions (6) through (9) by the same methods used to calculate ΔH_{10} and ΔH_{11}. For reaction (10) entropy changes of -13, -13 and -12 eu/mole are combined to give $\Delta S_{10} = -13 \pm 2$ eu at 1500°K. For reaction (11) the values are 6.2 and 6.5 eu to obtain as the best estimate $\Delta S_{11} = 6 \pm 1$ eu/mole. ΔS_6, ΔS_{10}, and ΔS_{11} are combined with the JANAF[10] entropies at 1500°K for $B_2O_3(\ell)$ and BeO(c) to give the remaining entropies in Table VI.

It should be noted that our value of $S_{1500} = 101$ eu for $B_2O_3(g)$ compares well with sommer, White, Linevsky and Mann's value $S_{1500} = 100.2$ eu. The model assumed by these authors is that of a V-shaped molecule.

5.4 Al-B-O System

The alumina-boric oxide system has been examined by Mallard,[20] Scholze,[21] and Baumann and Moore,[22] all of whom measured optical data, X-ray parameters and composition of the mixed oxide. Mallard, the first investigator, reported the constitution of the mixed oxide to be $Al_6B_2O_{12}$. Baumann and Moore, and later Scholze, found the

compound to have the composition $Al_{18}B_4O_{33}$. Scholze detected, in addition, the presence of a second compound $Al_4B_2O_9$. He found that both compounds are rhombic and melt incongruently, $Al_{18}B_4O_{33}$ at 1440°C, and $Al_4B_2O_9$ at 1050°C.

While the two condensed mixed oxides have been characterized in X-ray studies, there is no data at all relating to gaseous species or to thermodynamics of condensed or vapor phases. We have studied this system by measuring vapor pressures by Knudsen effusion, using a vacuum balance and mass spectrometer. The results of this research and the derived thermal properties are reported here.

5.4.1 B_2O_3 Pressure as a Function of Composition

The B_2O_3 pressure (B_2O_3 constituted over 99% of the vapor) was measured as a function of composition at constant temperature. This was achieved by measuring the weight change with time of a Knudsen cell containing B_2O_3 rich samples. As the B_2O_3 was lost the sample became richer in Al_2O_3. Constant pressures should indicate two-phase regions, while a decrease in pressure should occur at the phase boundary.

A number of measurements were made with mixtures of Al_2O_3 and B_2O_3 at temperatures from 990 to 1285°C using orifices from 10^{-2} to 5×10^{-4} cm^2. With the temperature at 1054°C and above, no change in B_2O_3 activity was observed up to 75% Al_2O_3. From this composition to 82% Al_2O_3 the pressure of B_2O_3 dropped and the sample appeared to stop losing weight. In none of these measurements was a second plateau observed after the decrease in activity Subsequent measurements described below indicate that the activity should have dropped to about 10^{-2} and the measurements for the largest orifices (because of a low evaporation coefficient) should have decreased to about 10^{-3} times that over B_2O_3. The rate of effusion at these lower pressures (10^{-8} to 10^{-9} atm) was too slow to detect under our experimental

conditions.

In a measurement at 990°C, a decrease in activity was observed at 67% Al_2O_3. The activity at 70% Al_2O_3 was about 0.4. The temperature was increased to 1057°C where the activity rose to unity and then decreased above 77% Al_2O_3 to 0.012 at 87% Al_2O_3.

These experiments confirm the existence of the two mixed oxides found previously, $Al_4B_2O_9$ (67% Al_2O_3) and $Al_{18}B_4O_{33}$ (82% Al_2O_3).

5.4.2 Pressure over $Al_{18}B_4O_{33}$-Al_2O_3

Pressures were measured over the pseudo-binary system $Al_{18}B_4O_9$-Al_2O_3. These experiments were carried out in the induction furnace shown in Fig. 2. The platinum cell was suspended directly in the work coil rather than using a target.

Two sets of measurements were made. First a charge of 69 mg $Al_{18}B_4O_{33}$ and 18 mg Al_2O_3 was added to a 1/4" dia. platinum cell with an orifice of 2.4×10^{-4} cm^2. Temperatures were measured on the platinum surface and were later corrected for the measured emissivity of the cell ($\epsilon = 0.31$). A number of isothermal measurements were made. These are given in Table VII and plotted in Fig. 10.

In the second set of measurements, a hole was drilled in the side of the cell without altering the remaining sample. This hole was designed to measure emissivity and to determine the effects of orifice size. The combined orifice areas, corrected for the Clausing factor were 7.8×10^{-3} cm^2. This combined area is 32 times larger than that of the original tope orifice. The results are given in Table VII and plotted in Fig. 10.

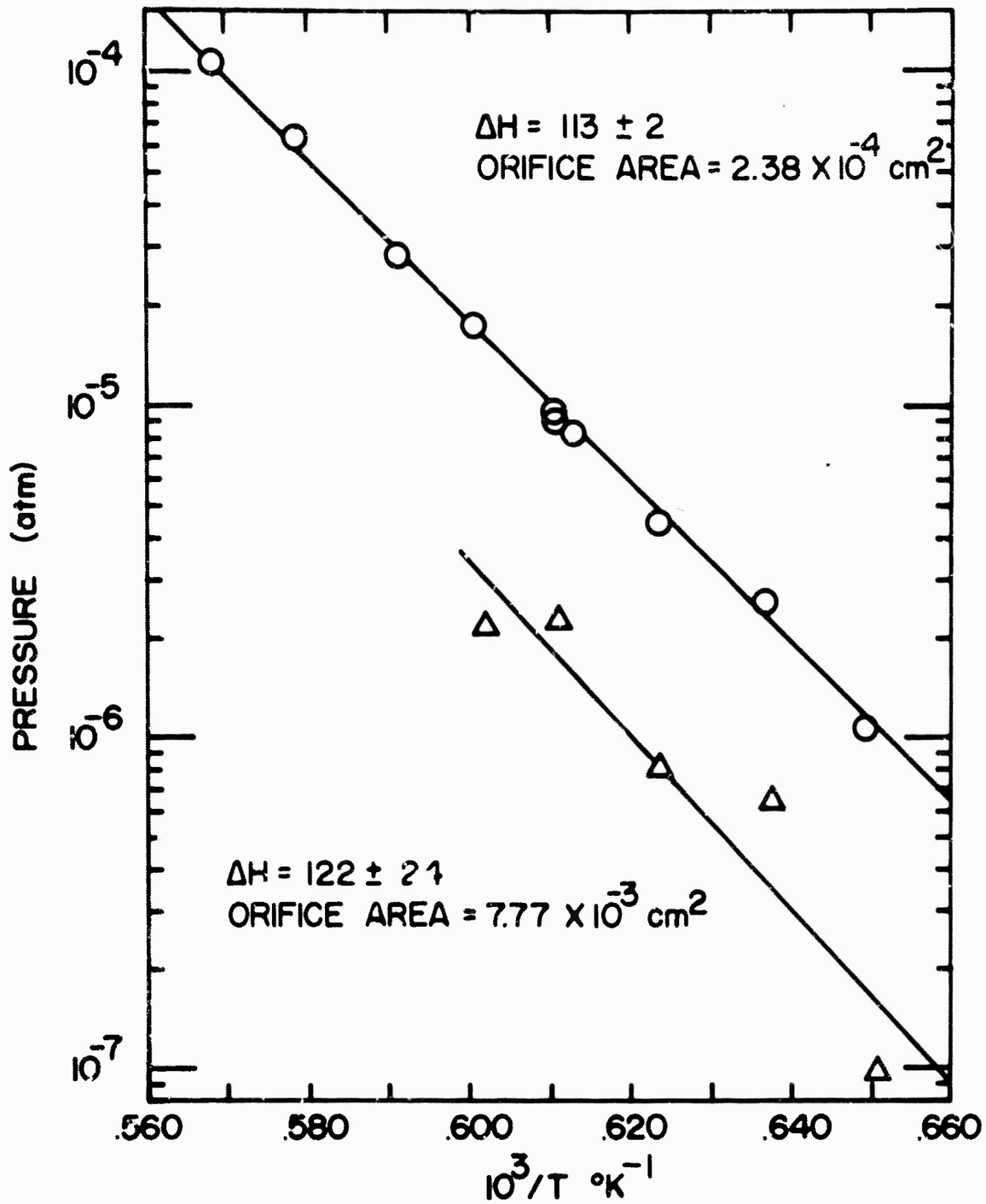

FIGURE 10 B_2O_3 PRESSURES OVER $Al_{18}B_4O_{33}$ + Al_2O_3

EFFECT OF ORIFICE SIZE

TABLE VII

B_2O_3 Pressure over $Al_{18}B_4O_{33} + Al_2O_3$

T, °K	Time, sec	Weight loss, μg	Effusion rate, $g\text{-}cm^{-2}\text{-}sec^{-1} \times 10^6$	Press. atm. $\times 10^6$
Orifice a				
1638	2,400	50	87.5	9.56
1638	2,700	55	85.5	5.03
1690	975	60	285.	28.6
1663	1,650	60	158.	17.4
1603	6,600	65	41.3	4.47
1570	8,400	48	24.0	2.57
1540	10,800	25	9.72	1.03
1632	3,600	64	74.7	8.15
1728*	1,500	200	560.	62.9
1759*	2,250	510	952.	108.
Orifice b				
1538	15,000	106	0.912	0.0956
1603	1,650	83	6.49	0.702
1568	3,450	161	6.02	0.644
1636	7,300	1260	20.8	2.28
1661	24,600	3710	19.5	2.16

a. Area corrected for Clausing factor = 2.38×10^{-4} cm^2

b. Area corrected for Clausing factor = 7.77×10^{-3} cm^2

* Above melting point of $Al_{18}B_4O_{33}$

In treating the data for orifice effects, use is made of the simplified Motzfeldt[5] equation to establish the magnitude of the evaporation coefficient. In this equation,

$$P_m = P_{eq} - \frac{aW_a}{B\alpha_e} P_m \qquad (13)$$

P_m and P_{eq} are the measured and equilibrium pressures, a and W_a are the orifice area and its Clausing factor, B is the sample area and

α_e is the evaporation coefficient.

The orifice area effects are quite large, indicating a very small evaporation coefficient for this system. The value for $1/B\alpha_e$ in equation (13) is 800. Inasmuch as the effective area of the powdered sample B cannot be established, it is only possible to state that α_e is less than 4×10^{-3}. This is the upper limit for α_e calculated for a solid, non-porous, plane sample. Even with an orifice area as small as 2.4×10^{-4} cm^2, the measured pressures must be increased 20%. From earlier measurements on this system, where the sample was heated until no further weight was lost, the weight of the residue was that of the Al_2O_3 initially present. Mass spectrometric data show that only B_2O_3 is present in the vapor. The data in Table VII were calculated on this basis.

The heat of reaction calculated by least squares for

$$1/2\ Al_{18}B_4O_{33}(c) \rightarrow 9/2\ Al_2O_3(c) + B_2O_3(g) \qquad (14)$$

is 113 ± 2 kcal/mole of B_2O_3, and the entropy change for this reaction is 47 ± 1 eu/mole of B_2O_3 where a correction has been made for the orifice effect. If the corresponding values for B_2O_3 are ΔH_{1500} = 93 ± 3 kcal/mole and ΔS_{1500} = 40 ± 1 eu/mole, then the thermal values for the reaction

$$2B_2O_3(\ell) + 9Al_2O_3(c) \rightarrow Al_{18}B_4O_9(c) \qquad (15)$$

are ΔH_{1500} = -42 ± 5 kcal/mole of $Al_{18}B_4O_{33}$ and ΔS_{1500} = -14 ± 3 eu/mole of $Al_{18}B_4O_{33}$.

This same system was studied with a mass spectrometer to establish the vapor composition. At temperatures up to 1740°K only $B_2O_3^+$ and its fragments were found. The second-law heat for reaction

(14) was ΔH = 112 ± 1 kcal/mole B_2O_3, in excellent agreement with the gravimetric measurements.

No aluminum-containing species were detected. An estimate of $\Delta H_{f\ 1500}$ (-504 kcal) and S_{1500} (158 eu) for $Al(BO_2)_3(g)$ indicate that this species, if it exists, would have a pressure at 1740°K, below our sensitivity. Our data for $AlBO_2(g)$ below also indicate that it will not be detected.

5.4.3 Pressure over $Al_4B_2O_9$-$Al_{18}B_4O_{33}$

Since $Al_4B_2O_9$ decomposes above its melting point of 1050 ± 20°C it was necessary to measure pressures below this temperature. The low evaporation coefficient ($< 4 \times 10^{-3}$) found for $Al_{18}B_4O_{33}$ requires a very small orifice to assure equilibrium conditions. These two conditions made it necessary to use the mass spectrometer with its greater sensitivity rather than the vacuum balance.

A series of measurements was first made in a 1/4" platinum cell having an orifice area of 2.4×10^{-4} cm^2 at temperatures below the melting point. A second set of experiments was then carried out both above and below 1050°C. These data are shown in Fig. 11. Past experience has shown that $Al_4B_2O_9$ disproportionates to B_2O_3 and $Al_{18}B_4O_{33}$ above 1050°C and the reverse reaction is exceedingly slow. It is assumed that all measurements after the melting point has been passed are on the two-phase system B_2O_3-$Al_{18}B_4O_{33}$.

A least squares fit to the first set of data was forced to intersect the second set at the melting point (1050°C). This gives for

$$9/5\ Al_4B_2O_9(c) \rightarrow 2/5\ Al_{18}B_4O_{33}(c) + B_2O_3(g) \qquad (16)$$

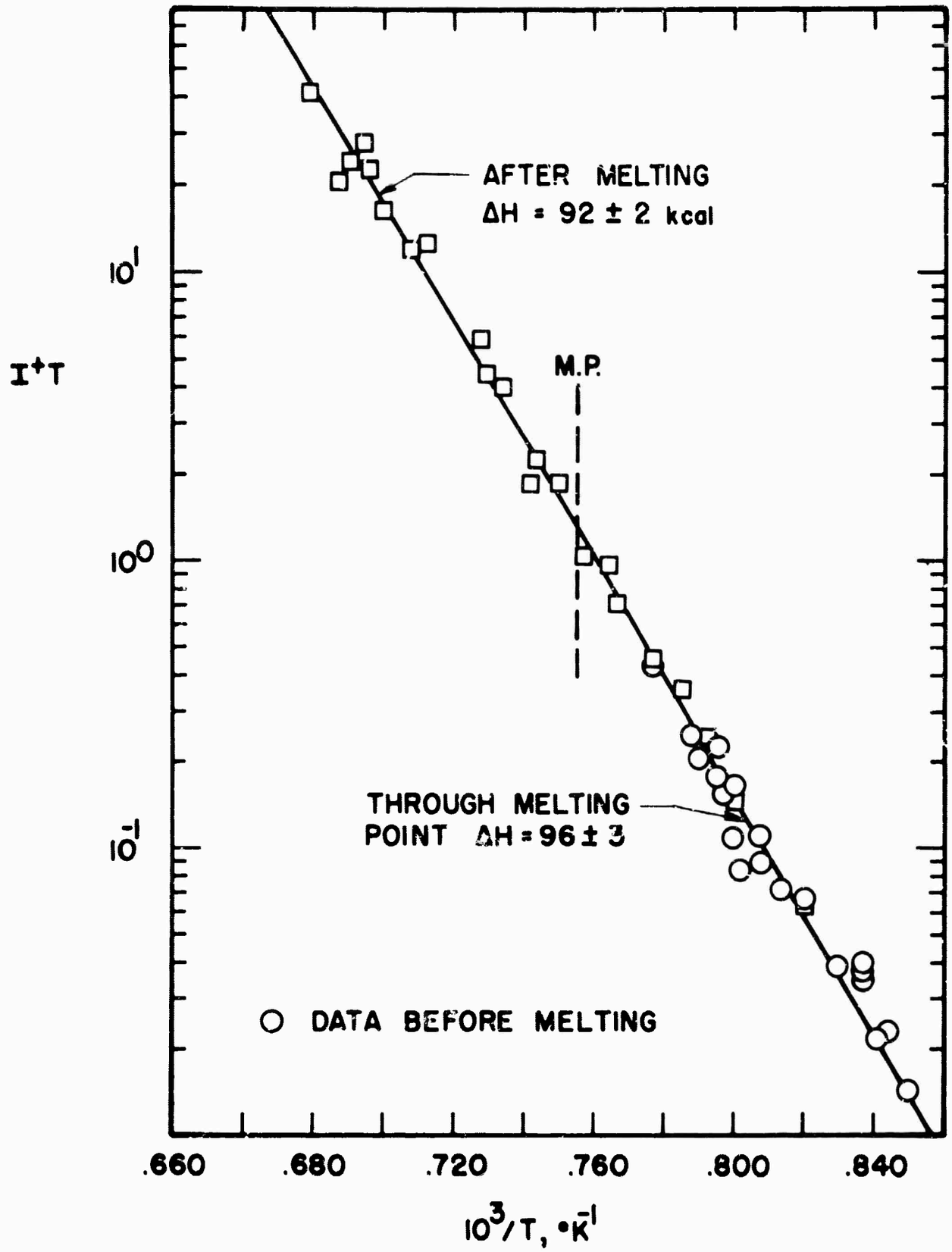

FIGURE 11 B_2O_3 PRESSURE OVER $Al_4B_2O_9$-$Al_{18}B_4O_{33}$

ΔH_{1250} = 95.9 ± 3.0 kcal/mole of B_2O_3 and ΔS = 43.0 eu/mole of B_2O_3. A second set of data yields for

$$B_2O_3(\ell) \rightarrow B_2O_3(g) \qquad (17)$$

ΔH_{1250} = 92.7 ± 1.7 kcal/mole and ΔS = 40.5 eu/mole where the entropy change is taken from B_2O_3 pressures found by gravimetric experiments. These data when combined with the heat and entropy of formation of $Al_{18}B_4O_{33}$ shown above give for

$$2Al_2O_3(c) + B_2O_3(\ell) = Al_4B_2O_9(c) \qquad (18)$$

ΔH_{1250} = -12 ± 2 kcal/mole of $Al_4B_2O_9$ and ΔS_{1250} = -4.5 ± 1 eu/mole of $Al_4B_2O_9$.

No aluminum-containing vapor species were found over this pseudo-binary system.

5.4.4 Pressures over $B_2O_3 + Al_2O_3 + Al$

A tungsten oxide Knudsen cell was loaded with Al_2O_3, B_2O_3 and Al powder in ratios to give Al:B:O of 1:1:2, and heated in the molybdenum crucible using a liner of platinum to prevent reaction between Al_2O_3 and Mo. The aluminum oxide cell orifice area corrected for the Clausing factor was 5 x 10^{-4} cm^2. The data are plotted in Figs. 12 and 13 and second-law heats are given in Table VIII. $AlBO^+$ appears to be a fragment of $AlBO_2^+$.

Boric oxide enriched with 96% isotopic B^{10} was used. This was necessary to separate the species Al_2O, $AlBO_2$ and B_2O_3, which all have a mass of 70, when composed of the normally more abundant B^{11}.

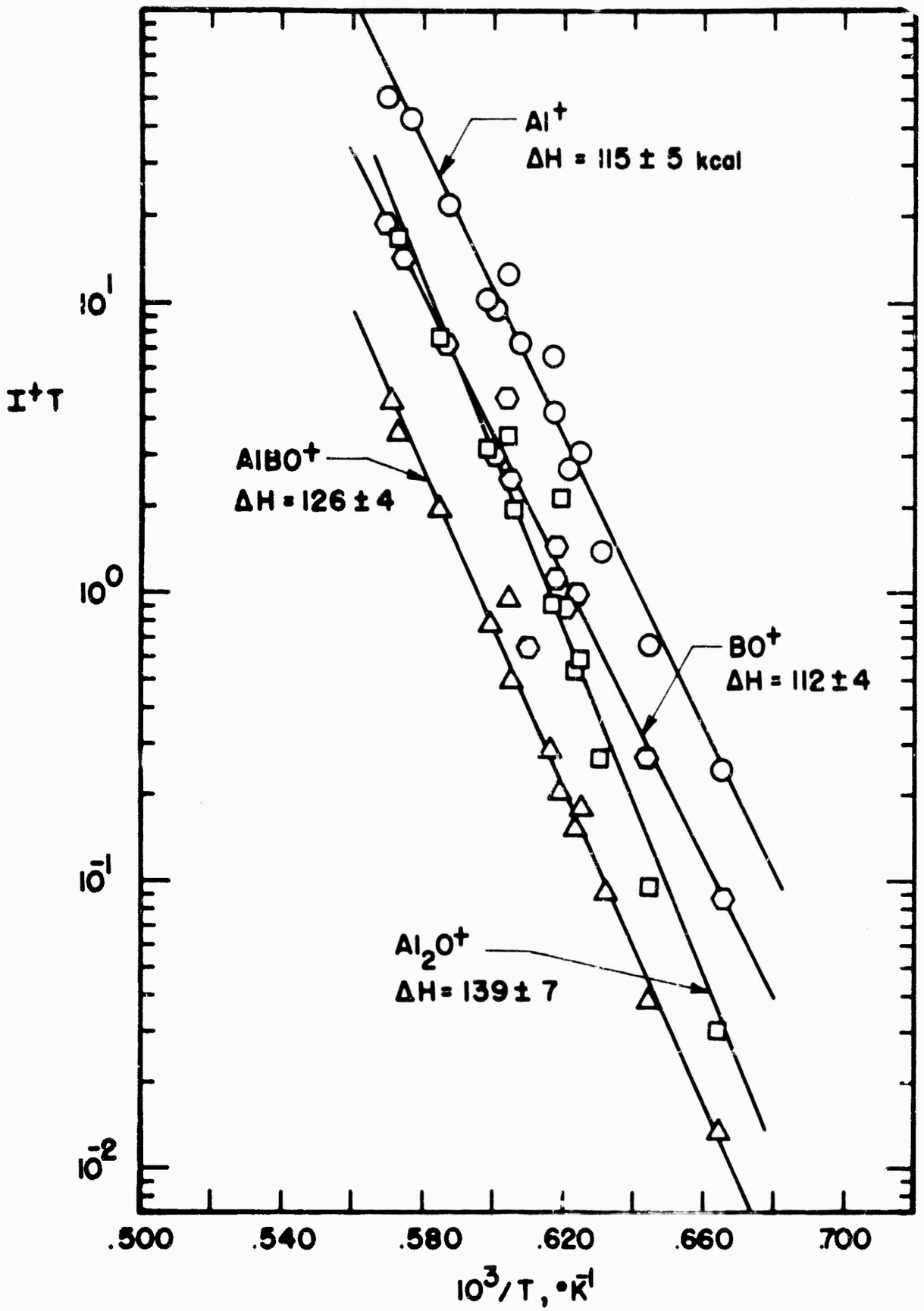

FIGURE 12 VAPOR SPECIES OVER THE Al-B-O SYSTEM

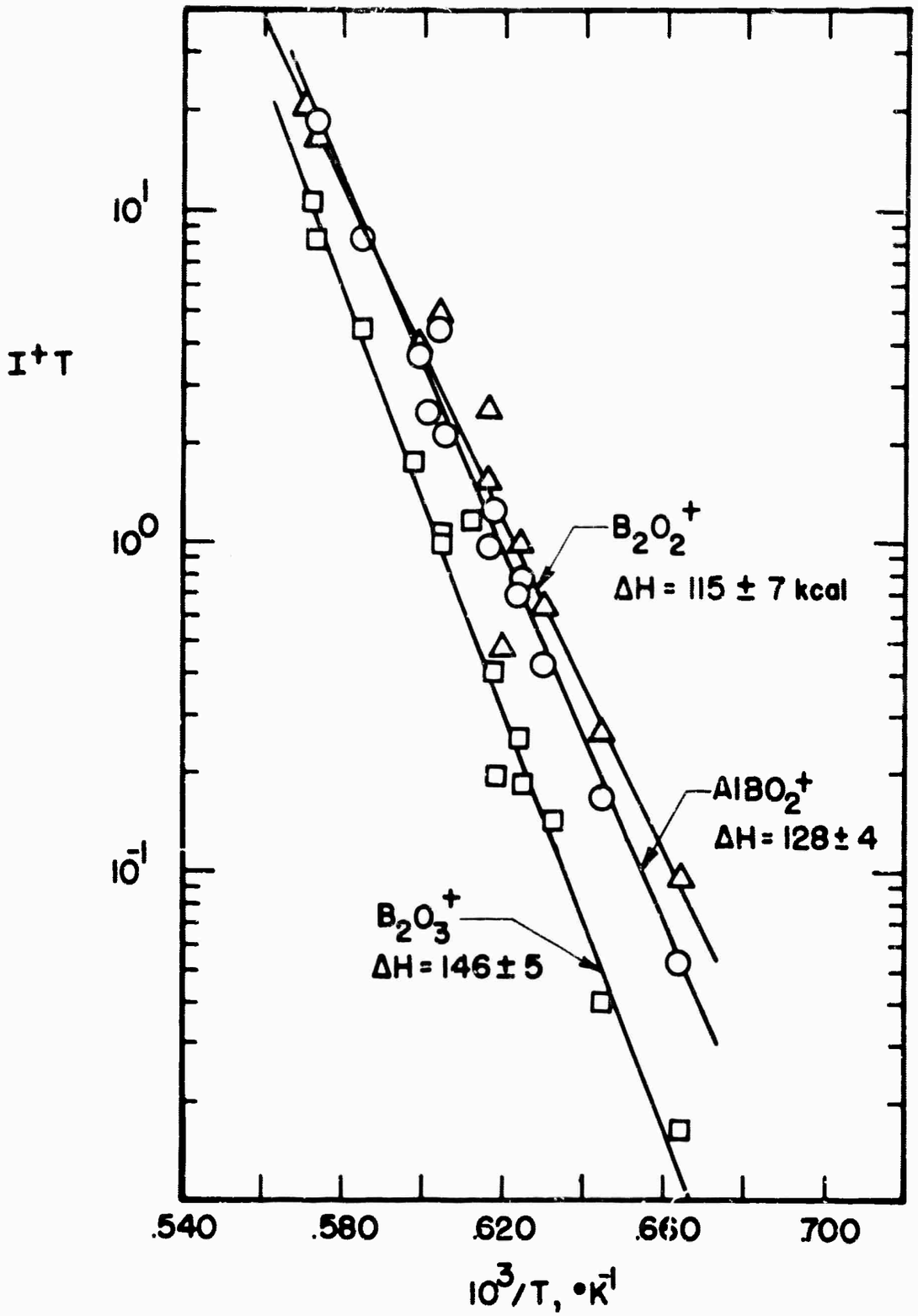

FIGURE 13 VAPOR SPECIES OVER THE Al-B-O SYSTEM

TABLE VIII

Second-Law Heats of Vaporization of Vapor Species over the Al-B-O System

Vapor Species	ΔH_{1500} kcal/mole
Al	115 ± 5
B_2O_2	115 ± 7
BO	112 ± 4
Al_2O	139 ± 7
$AlBO_2$	128 ± 4
B_2O_3	146 ± 5

Due to uncertainties about the condensed phases in this system, it is not possible to write the solid vapor reactions which were measured. However, the gas reaction may be used to determine the heat of formation of $AlBO_2(g)$. For the reaction,

$$1/2\ Al_2O(g) + 1/2\ B_2O_3(g) = AlBO_2(g) \qquad (19)$$

variation in the equilibrium constant with temperature is used to determine the heat of reaction. A least squares fit gives a second-law heat -18.2 ± 3.6 kcal/mole of $AlBO_2$ for reaction (19). From the JANAF Tables $\Delta H_f(1500)$ is -42.6 kcal/mole of $Al_2O(g)$ and $\Delta H_f(1500)$ is -200.8 kcal/mole of $B_2O_3(g)$. Combining these values we calculate $\Delta H_f(1500)$ = -140 ± 4 kcal/mole of $AlBO_2$.

The heats in Table VIII may be used to eliminate as condensed phases $Al(\ell)$, $B_2O_3(\ell)$, $Al_4B_2O_9$ and $Al_{18}B_4O_{33}$. The heat of vaporization $Al(\ell)$ to $Al(g)$ is 73 kcal[10] while $B_2O_3(g)$ should have a heat of 92, 96 and 113 kcal from $B_2O_3(\ell)$, $Al_4B_2O_9$ and $Al_{18}B_4O_{33}$. Our ratios of $B_2O_2(g)$ to $B_2O_3(g)$ are higher than those found by Inghram, Porter and Chupka,[23] and the heats of vaporization measured here are also higher,

115 and 146 kcal compared to Inghram, Porter and Chupka's values of 94 ± 8 and 92 ± 8. Our ratios of Al(g) to Al_2O(g) at 1500°K are nearly identical with those of Porter, Schissel and Inghram.[24] These authors measured pressures over Al + Al_2O_3. In the earlier work of Brewer and Searcy[25] on Al + Al_2O_3 there was less precision in the ratios of the gases, but the ratios are within a factor of 4 of Porter, Schissel and Inghram. The aluminum pressures measured by each of these authors are considerably less than that over pure Al, indicating the existence of aluminum suboxides. Hoch's high temperature X-ray data[26] indicate that Al_2O is the suboxide of aluminum which exists in the temperature range of the present work.

A calculation of the heat of reaction for

$$4/3\ Al + 1/3\ Al_2O_3 = Al_2O(g) \qquad (20)$$

with values from the JANAF Tables[10] yields a heat of 92 kcal which may be compared to our measured value of 139 kcal. Our higher heat would indicate that some other reaction is involved.

5.5 Rhenium

Rhenium is the only refractory metal which has a sufficiently low pressure and low reactivity with very stable oxides to be suitable for their study. Only two other metals have a lower vapor pressure, W and Ta. Both of these metals have the disadvantage of reacting with the two oxides under study, Al_2O_3 and BeO, forming either mixed tungsten oxides or TaO(g). Tantalum may also dissolve oxygen as well as forming mixed tantalum oxides. Rhenium apparently will not reduce either Al_2O_3 or BeO. Extrapolation of Coughlin's[27] tables for Re_2O_7(g) and ReO_3 to the temperature (2500°K) where the Al_2O_3 or BeO pressures may be measured indicates that the partial oxygen pressure is too low for reaction. A fourth possible cell for the study of these oxides, iridium, is more stable but has a much higher vapor pressure and lower melting point.

The rhenium cell was fabricated by spark gap machining a 0.437 inch diameter rod supplied by the Rembar Company. A removable lid containing an orifice was machined to fit the cylindrical base. A hohlraum was drilled in the side for temperature measurements.

The 24-gram cell was degassed, losing 55 mg. Measurements were made by weighing a glass target at a number of temperatures with the vacuum balance. Comparison of the target gain to the sample loss established the fraction of vapor condensed on the target. From the individual target weight gains, the above fraction, the sample dimension, sample temperature and time at temperature, the pressure of rhenium was calculated. Pressures in the vacuum system were less than 3×10^{-6} torr with the sample at temperature. Temperatures, measured with an optical pyrometer, were corrected for window adsorption.

The data are summarized in Table IX. Heats of vaporization in Table X, were calculated using Stull and Sinke's free energy functions for the solid and gas. The average heat at 298°K is 184.5 ± 1.5 kcal/g-atom which agrees very well with the study on rhenium by Sherwood et al.[20] These authors found ΔH°_{298} = 185.7 ± 1.0 kcal/g-atom. Sherwood measured the evaporation rate of a rhenium filament using an optical pyrometer and the emissivity of rhenium to determine the temperature.

TABLE IX

Vapor pressure of Rhenium

T, °K	Time sec x 10^{-3}	Target gain µg	Sample* loss mg	Evap.** rate g-cm^{-2}-sec^{-1} x10^{7}	Pressure atm. x 10^{8}
2694	9.00	50	40.0	5.28	4.53
2731	4.20	30	24.0	6.78	5.86
2758	4.20	38	30.4	8.59	7.47
2787	4.80	60	48.0	11.9	10.3
2821	6.00	80	64.0	12.6	11.1
2847	3.60	50	40.0	13.2	11.7
2877	3.00	60	48.0	19.0	16.8
2905	3.00	110	88.0	34.0	31.1

*Fraction of total evaporated metal condensed on target is 1.25×10^{-3}

**Sample area = 8.42 cm^2

TABLE X

Heat of Vaporization of Rhenium

T, °K	-RlnP cal/deg	-Δfef cal/deg	ΔH°_{298} kcal/g-atom
2694	33.62	33.97	182.1
2731	33.09	33.94	183.1
2768	32.61	33.91	184.1
2787	31.97	33.89	183.6
2821	31.82	33.86	185.3
2847	31.72	33.84	186.6
2877	31.00	33.82	186.5
2905	29.78	33.80	184.7
		Avg.	184.5 ± 1.5

5.6 BeO Effusion Rate

Only two studies have been made on this system, one by Erway and Seifert[30] and one by Chupka and Berkowitz and Giese.[31] In the experiments by Erway and Seifert, a tungsten Knudsen cell was heated inductively and the vapor from $_4Be^7$-enriched BeO was collected on targets. The amount of BeO was determined by counting for radioactive Be. These authors found that the rate of deposition on a quartz target was 0.60 of that on a BeO target. Using the higher rate they found effusion rates about 35% below those calculated for vaporization to atoms.

Chupka, Berkowitz and Giese used a high temperature mass spectrometer. They calibrated their ion intensities for Be^+ and O^+ with the dissociation pressure of BeO from the heat of formation of BeO. The ratio of their relative ionization cross sections σ_O/σ_{Be} 0.4 of the ratio from Otvos and Stevenson.[18] In addition to Be and O, $(BeO)_n(g)$ with n varying from one to six was found. Their sample was run in a tungsten crucible and $WO_2(g)$, $WO_3(g)$ and mixed species of these molecules with polymers of BeO were discovered. At 2242°K, ignoring the tungsten species, their data give 71% atoms and 29% $(BeO)_n(g)$ by weight. Chupka et al. suggest that their lower

relative ionization cross section ratios might be in error and that $(BeO)_n$ concentration based on Otvos and Stevenson ratios could be as much as 2-1/2 times higher. Chupka speculates that Erway's data may be in error because of the latter's assumption that the vapor from BeO will condense with 100% efficiency on a BeO target.

The rhenium Knudsen cell just described was also utilized to measure the BeO effusion rate. The data are given in Table XI and plotted in Fig. 14. The total rate is calculated from the JANAF Tables[10] as is the rate to be expected if effusion were to occur only to the constituent atoms. Weight balance calculations indicate that less than 1% of the vapor contains rhenium species.

TABLE XI

Effusion Rate of BeO

T, °K	Target gain μg	Weight loss through top orifice, mg	Time sec x 10^3	Effusion rate* $g\text{-}cm^{-2}\text{-}sec^{-1} \times 10^6$
2309	111	3.35[a]	26.4	11.1
2358	170	5.15	21.0	21.4
2388	90	3.61[b]	8.4	37.7
2414	118	4.73	8.4	49.4
2232	30	1.20	25.2	4.18
2439	150	6.02	9.6	55.1
2516	226	9.40[c]	4.2	197
2464	122	5.08	4.8	92.9
2490	56	2.33	1.8	114

*Orifice area = 1.14×10^{-2} cm^2.

The fractions striking the targets are: a, 3.31×10^{-2}; b, 2.49×10^{-2}; c, 2.40×10^{-2}.

The JANAF data are based on the mass spectrometric data of Chupka, Berkowitz, and Giese.[31] Our data are in excellent agreement with the total effusion rate of these authors. We find no reason to expect the $(BeO)_n$ concentration to be significantly higher. Like Erway and Seifert, we found the vapor from BeO to have a condensation

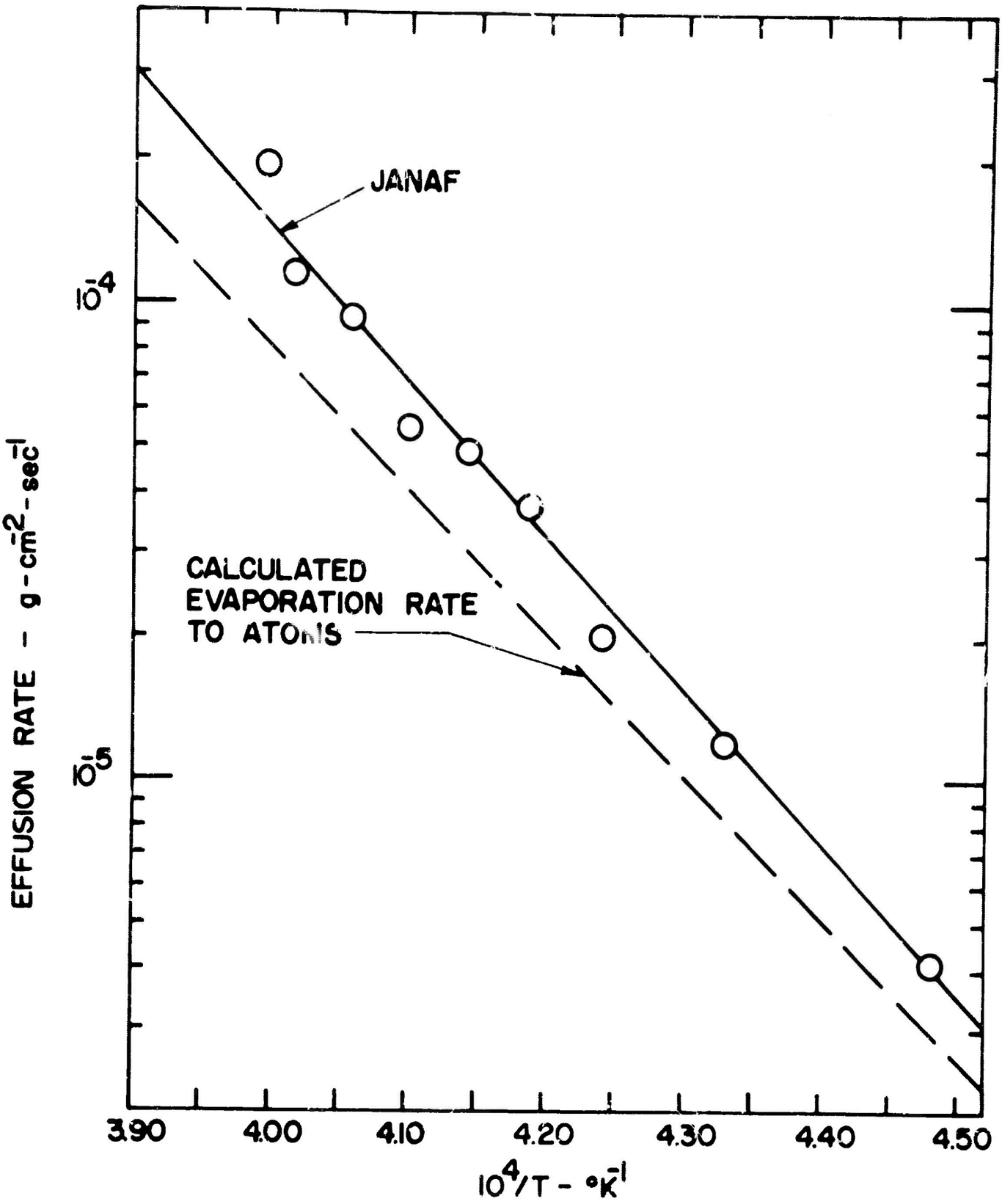

FIGURE 14 EFFUSION RATE OF BeO

coefficient of 0.57 on our glass targets. In experiments on BeO + Al_2O_3 the condensation coefficient was found to decrease from 1.0 for Al_2O_3 to 0.6 for 37 % Al_2O_3-63% BeO, remaining fairly constant up to 100% BeO. There is no data on mixed condensation of tungsten and beryllium oxides. It is possible that such mixtures have low condensation coefficients. However, our experience with BeO vapor condensing on glass agrees with Erway's BeO condensation on quartz and would seem to eliminate this as the explanation for the latter's low pressures.

5.7 Al_2O_3 Effusion Rate and Evaporation Coefficient

Drowart et al.[32] have established with a mass spectrometer that about 80% of Al_2O_3 vaproizes to the atoms, with the remainder vaporizing to Al_2O, AlO, and Al_2O_2. Brewer and Searcy[25] studied the vapor over Al_2O_3 + Al to give the oxide species. Brewer's data indicate that AlO and O should constitute the bulk of the vapor over Al_2O_3.

Gravimetric experiments have not established the relative amounts of the various species, but they may be used to determine the total effusion rate. This can be compared to the predicted rates.

Drowart et al. used Al_2C_3 liners in tungsten cells. Brewer and Searcy used tungsten and molybdenum cells without liners for Al_2O_3 vaporization. In the present study rhenium cells were used without liners. As discussed above, the rhenium should not reduce Al_2O_3. No data were found on aluminum solubility in rhenium.

To the cell described in Section 5.5 was added 20 mg of pure Al_2O_3 powder. This was vaporized at several temperatures until there was no further weight gain of the glass target. The target and cell were weighed with an analytical microbalance at the completion of the measurement. The fraction of vapor effusing from the top

orifice and condensing on the target was established from these weight changes, and the two orifices (top and side) were corrected for the Clausing factor.

The total weight loss of the cell was 24 mg, or 4 mg in excess of the Al_2O_3 added to the cell. The additional weight loss could be accounted for from the rhenium vapor pressures described in Section 5.5. Thus, within the precision of these measurements, Re does not react with Al_2O_3. Table XII gives the data and Fig. 15 shows the measured Al_2O_3 effusion rates compared to the rates computed from the JANAF Tables.[10] There is excellent agreement with the JANAF tables, indicating that the bulk of the oxide vaporizes to atoms of aluminum and oxygen.

TABLE XII

Effusion Rate of Al_2O_3

T, °K	Time, sec	Weight gain of target μg	Weight[a] loss through top orifice mg	Effusion[b] rate $g\text{-}cm^{-2}\text{-}sec^{-1} \times 10^6$
2411	10,200	100	3.39	29.0
2411	4,800	48	1.63	29.7
2464	6,600	116	3.93	52.2
2320	18,000	44	1.49	7.26
2361	19,200	88	2.98	13.6
2430	27,000	86	2.91	9.46
2389	24,000	104	3.53	12.9
2542	4,200	190	7.58	134.

a. Fraction striking target = 2.95×10^{-2}

b. Orifice area corrected for Clausing factor = 1.14×10^{-2} cm^2

A recent paper by Burns, Jason, and Inghram[33] reports a discontinuity in the evaporation rate of Al_2O_3 at its melting point. These authors found that a polycrystalline alumina rod evaporated about one-third as fast just below the melting point as it did immediately

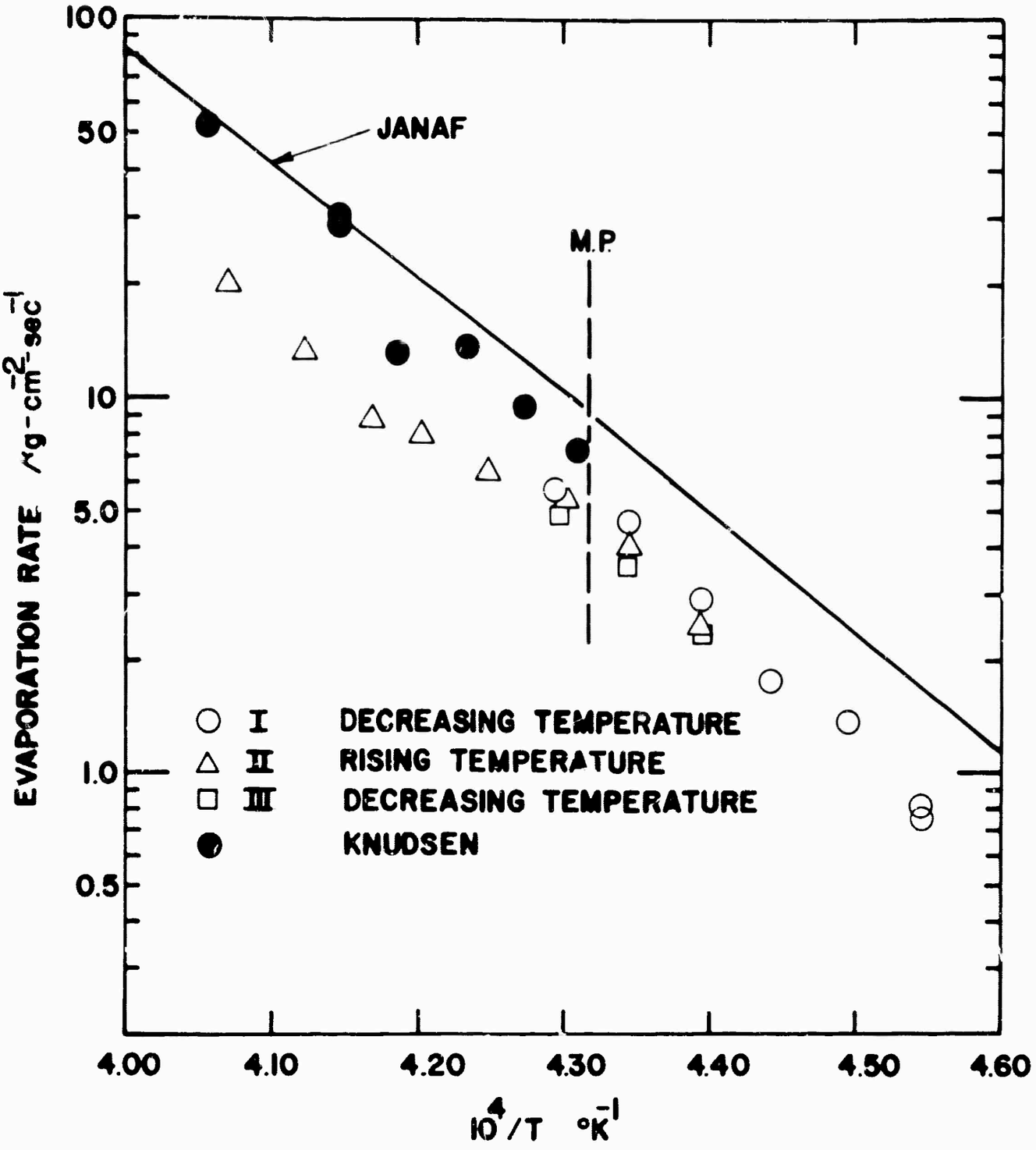

FIGURE 15 EFFUSION AND EVAPORATION OF Al_2O_3

above the melting point. Their method of heating the sample precluded continuous temperature measurements, although the point at which melting occurred was established through an optical pyrometer.

The present experiments were carried out in an open rhenium crucible heated inductively. This arrangement allowed us to measure temperature over the full range of the experiments. Three sets of tests were made. First, two sapphire rods were placed in the bottom of the crucible, which was heated initially to the expected melting point of Al_2O_3. This was followed at 25° intervals by successive lower temperature measurements. Evaporation rates were found by condensing the vapor on a target suspended from a recording vacuum balance. After several such experiments the crucible was removed from the system and examined. One rod had completely melted, while the second had partially melted. Thus the first measurement was made at the melting point of Al_2O_3. On our temperature scale, correcting for window adsorption and for a vertical thermal gradient of 25°, we find 2328°K as the melting point of Al_2O_3. This may be compared to 2315°K, the figure to be seen in the JANAF Tables[10] on Al_2O_3.

A second set of measurements was made starting below the melting point. Subsequently the temperature was dropped to the melting point and below.

The present data, when compared to our knudsen effusion measurements, indicate an evaporation coefficient between 0.5 and 1 for both liquid and solid Al_2O_3. That the evaporation rate falls farther below the effusion rate at higher temperatures may be due to larger thermal gradients with the open top.

Burns et al.[33] found an evaporation coefficient of unity for $Al_2O_3(\ell)$ and 0.3 for $Al_2O_3(c)$. Sears and Navais[34] believes that the evaporation coefficient of alumina is less than 3×10^{-4}, a

belief based on the fact that he did not find a deposit of evaporated Al_2O_3 or Al after heating his sample in vacuum. He estimates that 20 A of Al_2O_3 or 10 A of Al would be visible. Although we have had difficulty seeing the transparent Al_2O_3 on our glass cover slides with a deposit of 50 $\mu g/cm^2$ (about 2000 A), it is possible to see some contrast with an uncoated cover slide. It is interesting to note that 98% (i.e., within the precision of our measurements) of the Al_2O_3 calculated as striking the target, did in fact condense.

5.8 Al-Be-O

The effusion rates of three mixtures of Al_2O_3 and BeO — 66% BeO-34% Al_2O_3, 75% BeO-25% Al_2O_3 and 26% BeO-74% Al_2O_3 — were measured at 2415°K until each sample had been completely evaporated. All three mixtures are single phase liquids at 2415°K according to the phase diagram[35] constructed from Lang, Fillmore and Maxwell,[36] and from Galakhov.[37] The total effusion rate of each mixture is plotted versus time in Fig. 16, along with the calculated effusion rate of BeO(c) and $Al_2O_3(\ell)$.

It is evident that the beryllium rich samples lose BeO initially. The 26% BeO-74% Al_2O_3 sample vaporizes congruently at this temperature. From the total effusion rate and the fraction of the pure compounds vaporizing to the elements, we may calculate the Be, Al and O pressures over $BeO.3Al_2O_3(\ell)$. At 2415°K, 60% BeO and 72% Al_2O_3 vaporizes to their elements; the remaining percents vaporize as molecules.

Using the total effusion rate for this solution, 2.57×10^{-5} $g/cm^2/sec$, the following pressures are calculated: $P_O = 2.44 \times 10^{-6}$ atm, $P_{Al} = 1.93 \times 10^{-6}$ atm and $P_{Be} = 1.55 \times 10^{-1}$ atm. These pressures are for the reaction

$$BeO.3Al_2O_3(\ell) \rightarrow Be(g) + 6Al(g) + 10\ O(g) \qquad (21)$$

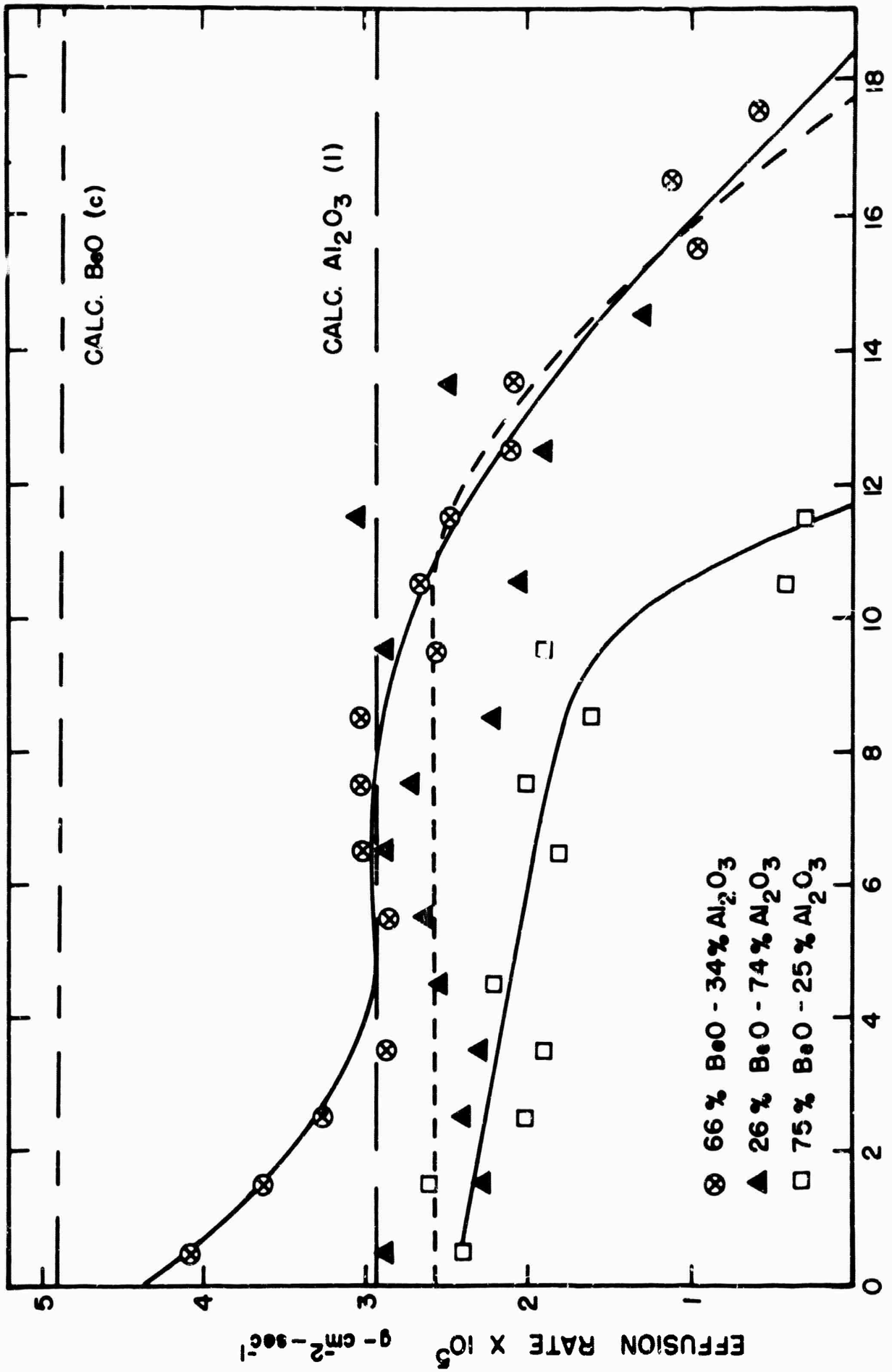

FIGURE 16 EFFUSION CURVES OF BeO-Al_2O_3 SOLUTIONS AT 2415°K

assuming $\Delta C_p = 0$ for $BeO(\ell) + 3Al_2O_3(\ell) \rightarrow BeO.3Al_2O_3(\ell)$, Δfef[10] for reaction (21) is -568.1 cal/deg at 2415°K. This gives $\Delta H_r°298$ = 2446 kcal. The $\Delta H_2°298$ for $BeO(\ell)$ is -129.6 kcal[10] and for $Al_2O_3(\ell)$ is -373.4 kcal. Combining these with the heat of formation of Al(g) 78.0 kcal,[10] O(g) 59.56 kcal and Be(g) 78.6 kcal,[10] we calculate for

$$BeO(\ell) + 3Al_2O_3(\ell) = BeO.3Al_2O_3(\ell) \qquad (22)$$

$\Delta H_r°298 = -54 \pm 15$ kcal or $\Delta H_f°298 = -1304 \pm 15$ kcal for $BeO.3Al_2O_3(\ell)$, and $\Delta H_f°298 = -1397 \pm 15$ kcal for $BeO.3Al_2O_3(c)$. It is assumed that the heat of fusion of the 1:3 compound is the sum of the heats of fusion of the individual oxides. The value found here does not agree with Young[38] who finds -0.8 kcal for the formation of $BeO.3Al_2O_3$ from the individual oxides. His value is based on the reaction of $BeO.3Al_2O_3$ with water to form $Be(OH)_2(g) + 3Al_2O_3$.

Our measurements indicate that samples with more BeO will not vaporize congruently. Efimenko's[36] mass spectrometric data on chrysoberyl ($BeO.Al_2O_3$) bears this out. The vapor over the 1:1 compound was very rich in beryllium (about 6 times that for congruent vaporization)and it slowly increased in aluminum content with time. From Efimenko's pressures for Al(g), Be(g), O(g) and AlBeO(g) at 2417°, we calculate that the AlBeO pressure over $BeO.3Al_2O_2(\ell)$ should be 2.4×10^{-9} atm. With this pressure and those calculated above for the elements and by using a free energy function of -72.2 cal/deg for AlBeO(g) we find that for

$$BeO.3Al_2O_3(\ell) \rightarrow AlBeO(g) + 5Al(g) + 9\ O(g), \qquad (23)$$

$\Delta H_r°298 = 2205 \pm 13$ kcal. The free energy function for AlBeO(g) is the average for that of Al_2O and Be_2O.[10] From our heat of formation for liquid $BeO.3Al_2O_3$ and from JANAF values for the elements, $\Delta H_f°298$ = -25 ± 13 kcal/mole AlBeO(g). The estimated uncertainty is based on our mean deviation for vaporization of Al_2O_3. Efimenko's data based

gas-phase reactions yield -17.5 ± 3.3 and -9.8 ± 6.2 kcal for the heat of formation of AlBeO(g). Since the heats of formation of $Be_2O(g)$ and $Al_2O(g)$ are -15.0 and -31.4 kcal/mole it seems reasonable to expect that AlBeO(g) should fall between these values.

5.9 $AlF_3(g)$ and AlF(g)

The pressure over AlF_3 and over AlF_3 + Al were measured in a 1/4" dia. boron nitride cell. Thermodynamic calculations indicate that AlF_3 should not react with BN. Although AlN is more stable than BN the formation of AlF(g) is much more liable to occur. BN should not react with BF_3. These studies were initiated as preliminary research for the investigation of the Al-B-F system.

The BN cell was degassed at 800°C (about 100° higher than the experiments. Of 96 mg of AlF_3, about 18 mg was lost before achieving a constant effusion rate. The high early measurements were rejected. The results of the later AlF_3 pressure measurement are given in Table XIII and third-law heats of vaporization are calculated in Table XIV. The data are plotted in Fig. 17. A least squares fit to the data give a second-law heat ΔH_{298} = 71.1 kcal, in good agreement with the JANAF value of 71.5 ± 1.5. Our third-law value is 72.7 ± 0.1 kcal.

TABLE XIII

AlF_3 Pressure over $AlF_3(c)$

T, °K	Time sec x 10^{-4}	Weight loss g x 10^4	Press.[a] atm. x 10^8
994	2.16	26.	449.
1022	3.78	16.6	162.
994	1.08	12.8	445.
1125	12.42	1.86	5.24
1125	7.02	1.04	5.20
1088	2.16	0.98	16.2
1055	1.08	1.52	51.2

a. Orifice area corrected for Clausing factor = 1.66 x 10^{-3} cm^2

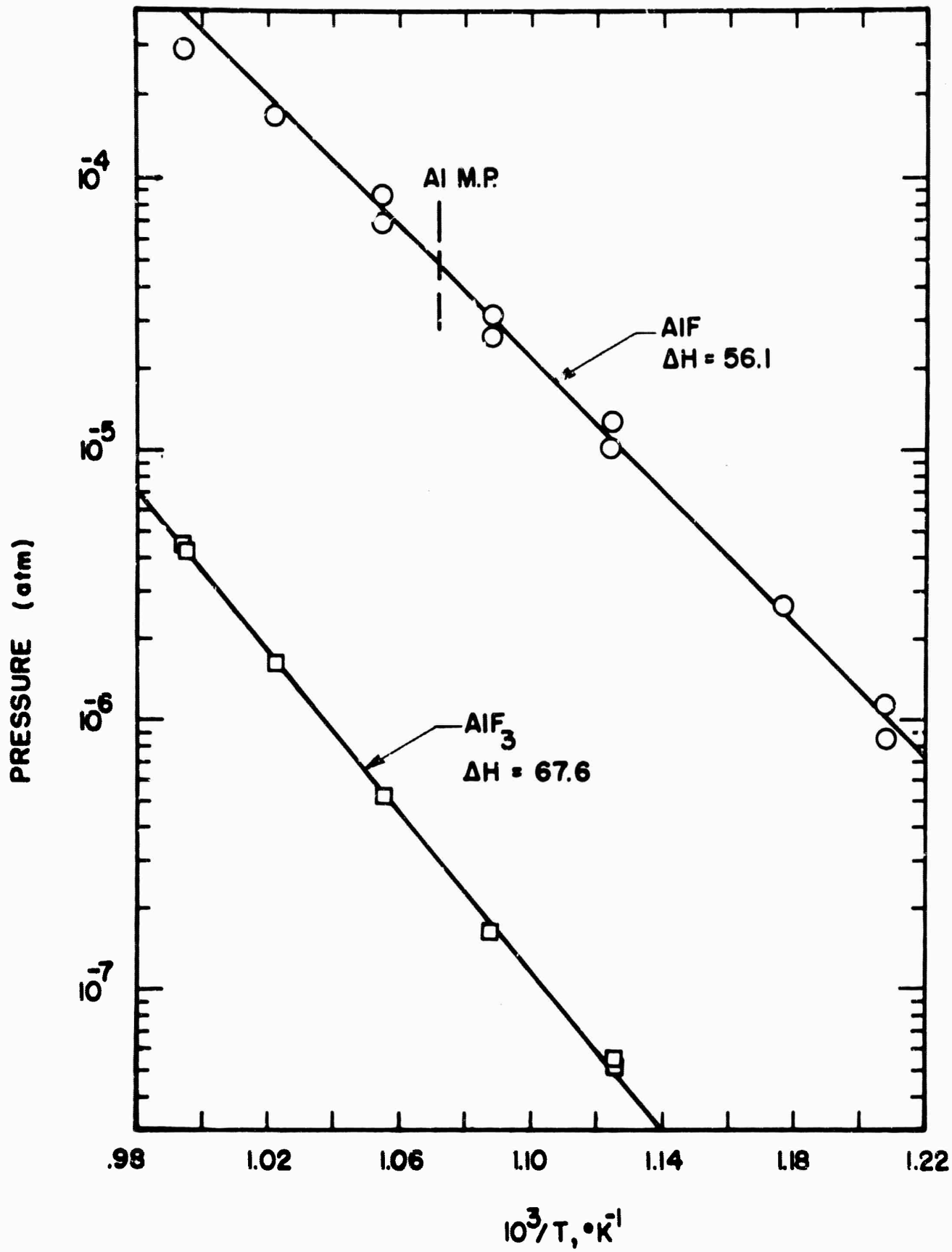

FIGURE 17 $AlF_3(g)$ OVER $AlF_3(c)$ AND $AlF(g)$ OVER AlF_3 + Al

TABLE XIV

Third-law Heat of Vaporization of AlF_3

T, °K	$-RlnP_{AlF_3}$ cal/deg	$-\Delta fef^b$ cal/deg	ΔH°_{293} kcal/mole
994	24.47	47.84	72.74
1022	26.50	47.96	72.82
994	24.49	47.84	72.76
1125	33.32	48.30	72.56
1125	33.33	48.30	72.57
1088	31.07	48.18	72.83
1055	28.79	48.07	72.86
		Avg.	72.7 ± 0.1

b. From JANAF Tables

Using the remaining AlF_3 sample with Al powder, AlF pressures were measured. These results are given in Tables XV and XVI, and Figure 17. A least squares fit to the data below the melting point of aluminum (832°K) gives a second-law of ΔH_{298} = 58.3 kcal which may be compared to our third-law value ΔH_{298} = 56.0 ± 0.2 kcal for

$$1/3\ AlF_3 + 2/3\ Al = AlF(g) \qquad (24)$$

From the later value and JANAF data we calculate $\Delta H^\circ_f 298$ of AlF(g) = -63.3 ± 0.7 kcal/mole.

TABLE XV

AlF Pressures over Al + AlF_3

T, °K	Time sec x 10^{-2}	Weight loss g x 10^4	Pressure[a] atm. x 10^7
1006	12	55.0	2910.
889	24	5.10	127.
828	54	0.800	8.52
919	30	15.8	320.
948	12	17.0	874.
828	486	9.80	11.3
850	108	5.00	27.0
889	48	8.10	101.
919	24	10.3	260.
948	12	13.4	690.
978	6	16.0	1670.

a. Orifice area corrected for Clausing factor = 1.66 x 10^{-3} cm^2

TABLE XVI

Third-law Heat of Vaporization of AlF(g) from Al + AlF_3(c)

T, °K	$-R\ln P_{AlF}$ cal/deg	$-\Delta fef$[b] cal/deg	ΔH_T° (298) kcal/mole of AlF(g)
1006	16.18	38.18[c]	56.09[c]
889	22.40	40.23	55.68
828	27.78	40.40	56.45
919	20.57	40.14	55.79
948	18.57	38.35[c]	55.66[c]
828	27.21	40.40	55.98
850	25.84	40.34	55.95
889	22.86	40.23	56.09
919	20.98	40.14	56.17
948	19.04	38.35[c]	56.11[c]
978	17.28	38.26	56.02[c]
		Avg.	56.0 ± 0.2[d]

b. From JANAF Tables

c. Above melting point of Al - corrected for ΔH_{fus} of Al

d. This value and JANAF data yield $\Delta H_f^\circ 298$ = -63.3 ± 0.7 kcal/mole AlF(g).

5.10 Preliminary Results on the Al-B-F System

The BN cell containing AlF_3 + Al was heated in static pressures of BF_3 (about 10 torr) until the sample stopped losing weight. From the volume of the system and the weight loss, the pressure of $AlBF_4$ was calculated. We have assumed that the free energy functions for $AlBF_4$ are essentially the same as those given in JANAF[10] for AlF_4. Two preliminary measurements are given below for

$$1/3\ AlF_3(c) + 2/3\ Al(c) + BF_3(g) = AlBF_4(g) \qquad (25)$$

T, °K	$-RlnP_{BF_3}$	$-RlnP_{AlBF_4}$	$-\Delta fef$ cal/deg	ΔH°_r 298* kcal	ΔH°_f 298** kcal
760	8.70	14.52	3.90	7.4	-396.8
650	8.93	13.11	4.10	5.4	-394.8

*Heat of reaction[25] ** Heat of formation of $AlBF_4$

More work is necessary to establish that no other reactions occur. Further experiments are also required to determine the effects of pressure and temperature. The values found here appear to be reasonable when compared to $AlLiF_4$. For example heats are calculated for

$$AlLiF_4(g) \rightarrow LiF(g) + AlF_3(g) \qquad \Delta H_{298} = 72 \text{ kcal}$$

and

$$AlBF_4(g) \rightarrow BF(g) + AlF_3 \qquad \Delta H_{298} = 82 \text{ kcal}$$

The latter reaction should require more heat since B has extra bonding electrons in contrast to Li which does not.

REFERENCES

1. C. N. Cochran, Rev. Sci. Instr. 29, 1135 (1958).

2. R. Speiser, S. Naiditch and H. L. Johnston, J. Am. Chem. Soc. 72, 2578 (1950).

3. A. Büchler and J. B. Berkowitz-Mattuck, J. Chem. Phys. 39, 286 (1963).

4. D. L. Hildenbrand, W. F. Hall and N. D. Potter, J. Chem. Phys. 39, 296 (1963).

5. K. Motzfeldt, J. Phys. Chem. 59, 139 (1955).

6. G. M. Rosenblatt, J. Electrochem. Soc. 110, 563 (1963).

7. J. P. Hirth and G. M. Pound, "Condensation and Evaporation," New York, MacMillan, 1963, p. 80.

8. G. Wyllie, Proc. Roy. Soc. (London) 197A, 383 (1949).

9. E. M. Mortensen and H. Eyring, J. Phys. Chem. 64, 846 (1960).

10. JANAF Thermochemical Tables, Thermal Laboratory, Dow Chemical Company, Midland, Michigan.

11. L. Brewer and D. Mastick, J. Chem. Phys., 19, 834 (1951).

12. R. F. Porter, W. A. Chupka and M. G. Inghram, J. Chem. Phys. 23, 216 (1955).

13. J. F. Kincaid and H. Eyring, J. Chem. Phys. 4, 620 (1938).

14. H. Menzel and S. Slivinski, Z. Anorg. Allgem. Chem. 249, 357 (1942); H. Menzel and J. Adams, Glastech. Ber. 22, 237 (1949).

15. L. Ya. Mazelev, Isvest. Akad. Nauk Beloruss, S.S.R. No. 4, 105 (1953).

16. P. E. Blackburn, J. Phys. Chem. 62, 897 (1958).

17. O. Kubachewski and E. LL. Evans, Metal Physics and Physical Metallurgy, Pergamon Press, New York, 1958, p. 66.

18. J. W. Otvos and D. P. Stevenson, J. Am. Chem. Soc. 78, 546 (1956).

19. A. Sommer, D. White, M. J. Linevsky, and D. E. Mann, J. Chem. Phys. 38, 87 (1963).

20. E. Mallard, Compt. Rend. 105, 1260 (1887).

21. H. Scholze, Z. Anorg. Allgem. Chem. 284, 272 (1956).

22. H. N. Baumann, Jr. and C. H. Moore, Jr., J. Am. Ceramic Soc. 25, 391 (1942).

23. M. G. Inghram, R. F. Porter and W. A. Chupka, J. Chem. Phys., 25, 498 (1956).

24. R. F. Porter, P. Schissel and M. G. Inghram, J. Chem. Phys 23, 339 (1955).

25. L. Brewer and A. W. Searcy, J. Am. Chem. Soc. 73, 5308 (1951).

26. M. Hoch and H. L. Johnston, J. Am. Chem. Soc. 76, 2560 (1954).

27. J. P. Coughlin, "Contributions to the Data on Theoretical Metallurgy, XII. Heats and Free Energies of Formation of Inorganic Oxides, Bulletin 542, Bureau of Mines, 1954.

28. D. R. Stull and G. C. Sinke, Thermodynamic Properties of the Elements, American Chemical Soc., Washington, D. C., 1956.

29. E. M. Sherwood, D. M. Rosenbaum, J. M. Blocher, Jr., and I. E. Campbell, J. Electrochem. Soc. 102, 650 (1955).

30. N. D. Erway and R. L. Seifert, J. Electrochem. Soc. 98, 83 (1951).

31. W. A. Chupka, J. Berkowitz and C. F. Giese, J. Chem. Phys. 30, 827 (1959).

32. J. Drowart, G. DeMaria, R. P. Burns, and M. G. Inghram, J. Chem. Phys. 32, 1366 (1960).

33. R. P. Burns, A. J. Jason, and M. G. Inghram, J. Chem. Phys. 40, 2739 (1964).

34. G. W. Sears and L. Navais, J. Chem. Phys. 30, 318 (1959).

35. E. M. Levin, C. R. Robbins and H. F. McMurdie, Phase Diagrams for Ceramists, Ed. M. K. Reser, The American Ceramic Society, Columbus, Ohio, ' 64, p. 99.

36. S. M. Lang, C. L. Fillmore and L. H. Maxwell, J. Research Natl. Bur. Standards, 48 (4), 301 (1952); RP 2316.

37. F. Ya. Galakhov, Izvest. Akad. Nauk S.S.S.R., Otdel Khim. Nauk 1035 (1957).

38. W. A. Young, J. Phys. Chem. 64, 1003 (1960).

39. J. Efimenko, Natl. Bur. of Standards Report 8626, p. 25, January 1965.